



Changes and variability in rainfall onset, cessation, and length of rainy season in the IGAD region of Eastern Africa

Paulino Omoj Omay^{1,2} · Nzioka J. Muthama¹ · Christopher Oludhe¹ · Josiah M. Kinama¹ · Guleid Artan² · Zachary Atheru²

Received: 25 November 2022 / Accepted: 12 March 2023 / Published online: 24 March 2023
© The Author(s) 2023

Abstract

Rainfall onset dates (ROD), rainfall cessation dates (RCD) and length of rainy season (LRS) are crucial for crop production and food security in Eastern Africa yet scantily documented. This paper seeks to investigate the spatial patterns of these parameters. Data used are Climate Hazards Group InfraRed Precipitation with Station data (CHIRPS v2.0) and National Oceanic and Atmospheric Administration (NOAA) gridded temperature. Threshold of 1 mm for rainy day, 20 mm over 5 days with at least 3 rain days and dry spell not exceeding 7 days in the next 21 days were used to determine RODs. The Potential Evapotranspiration (PET) and Water Balance (WB) criteria were computed to determine RCDs. The differences between ROD and RCD were used in calculating LRS. The results showed early rainfall cessation over more than 30 counties in Kenya lead to shortened rainy season by 10–20 days during MAM season. Similarly, 20–40 days early onset dates are observed in most counties in upper Nile, Unity, and Jonglei states in South Sudan, while 20–40 days delayed rainfall onset was observed in Khartoum and southern parts of Nile state western Darfur, eastern and Aljazeera states in Sudan, most parts of Ethiopia and Eritrea districts during JJA season. Highlands of western and Nyanza region in Kenya, most parts of Uganda observed rainfall onset by March and no sign of cessation before November. Early cessation over northern Uganda districts was behind shortened LRS, furthermore, the early RODs over western and southwestern Uganda districts increased LRS. Prolonged dry conditions over northern Sudan, southeastern parts of South Sudan, northern Kenya, central Somalia, northern Darfour, Kordofan and northern parts of Sudan exacerbated by significant delayed onset and early cessation of rainfall. These findings are important for rain-fed agricultural planning and food security in the IGAD region of Eastern Africa.

1 Introduction

Rainfall is the most important climatic variable for planning and management of rain-fed agriculture over the Greater horn of Africa (Funk et al. 2008, Lyon and Dewitt, 2012, Mwangi, et al. 2014, Gudoshava et al. 2020a). The timing of onset, distribution, cessation, intensity, frequency, and length of growing period in east Africa plays a vital role for agricultural input. The gross domestic product (GDP) of most countries in the region are climate sensitive (Kandji and Verchot, 2014), which easily could be affected by change

and variability in rainfall onset dates (ROD), rainfall cessation dates (RCD) and length of rainy season (LRS) patterns (Camberlin et al. 2009). The long-term shifts in variability and changes in mean state of ROD, RCD, and LRS could add more uncertainty and difficulties in crop yield prediction which is primarily important in projections of food security crises (Kandji and Verchot, 2014).

Agriculture plays a vital role in the lives of the people of East Africa, with around 80% of the population being engaged in agriculture activities (Recha et al. 2012). The smallholder farmers depend on the rain-fed farming of food crops (i.e. maize, wheat, sorghum, rice) or cash crops such as sugarcane, tea, cotton, coffee among others (Kirina et al. 2022). With continuation of anthropogenic activities and Global warming (GW), it is expected, the pattern of ROD, RCD and LRS has changed in the past, present time, and will continue in the future. The total rainfall patterns and long-term trends in most cases are driven by changes and variability in intra-seasonal rainfall characteristics (Camberlin

✉ Paulino Omoj Omay
paulinoomay@gmail.com

¹ Department of Earth and Climate Sciences, Faculty of Science & Technology, University of Nairobi, Nairobi, Kenya

² IGAD Climate Prediction and Application Centre (ICPAC), Nairobi, Kenya

et al. 2009). The study by Wainwright et al. (2019a) inferred that rainfall decline over east Africa is due to late onset dates and earlier cessation leading to shortening of the rainy season. This shed light on some reasons behind the past and current rainfall trend, which indicated the decline was due to change and variability in rainfall intensities. Also studies in the region highlighted the observed increase in mean state of extreme rainfall events such as drought over east Africa associates with delayed onset, early withdrawal of rain and reduced rainfall intensity (Camberlin et al. 2009, Haile et al. 2020), prolonged dry spells (Gitau et al. 2013).

The IGAD region is characterized by year-to-year variation in climate and different opportunities of agricultural seasons three times a year in some regions. These seasons are March, April, and May (MAM); June, July, August, and September (JJAS); and October, November and December (OND) seasons (Beltrando, 1990). The MAM and OND seasons are usually referred to as long and short rainy seasons within equatorial East Africa, while JJAS season is usually referred to as summer monsoon rains, which is called Kiremt in Ethiopia, and Kareef in both Sudan and South Sudan. The Kiremt account for 65–95% over Ethiopia (Segele and Lamb, 2005) and Kareef rains account for 80–95% over South Sudan (Omoj et al. 2016) and 95–99% of total annual rainfall over Sudan. The spatial and temporal characteristics of RODs, RCDs, and LRSs play a significant role in agriculture planning and main staple food production stability (Kumar et al. 2012), crop growth and food security (Chemura et al. 2020). Also, contribute directly in availability of the necessary water for food and cash crops production (Upriety et al. 2019). In addition, RODs, RCDs and LRSs patterns drive agricultural preparations such land clearance, tilling of soil, planting, and good harvest depends on knowing timing of planting and cropping which governs by nature of rainfall onset and cessation dates (Yashim et al. 2020). Furthermore, these patterns contribute directly or indirectly on other consumable inputs such as labour, soil type, fertilizers, insecticides, and capital inputs such as mechanical and technology used to maximize yields of grains, seeds and nuts, vegetables and fruits been consumed or profitable cash crops for small-scale farms (Lobell and Burke, 2009).

The baseline information on rainfall intensity, rainfall distribution and onset dates are fundamental for farmers to avoid confusions and losses of crop seeds and reduction in crop yield through wrong time cropping due to false rain onset (Yashim et al. 2020). Food crop farmers in Nasarawa State in Nigeria and many regions in Africa reported of having limited information on planting and harvesting dates, types of crops and seeds suitable when there is shifts in RCDs, RCDs, and LRS become longer or shorter under current and future climate conditions (Yashim et al. 2020). These situations could force farmers to rely on assumptions and mere guess work considered local indigenous

agricultural knowledge or farming by experience as a scaling strategy for climate-smart agriculture (Kirina et al. 2022). There is a need for sufficient, reliable, and timely spatial and temporal information on the mean state, changes, and variability in onset and cessation dates and length of rainy season patterns. This information could be potentially of great value leading to significant early warning building blocks, adaptation options, accurate decision-making such as adjusting planting dates, seeds varieties, and irrigation practices (Amarasingha et al. 2015).

The goal of this study therefore is to determine the patterns of changes and variability in RODs, RCDs and LRS for MAM, JJA, SON) and DJF in the IGAD region. This information could contribute to successful crop production (MacLeod, 2018), selection of the crop type and variety, timing of sowing, short-term seed storage and harvesting. The paper is structured as follows: Section 2 describes the CHIRPS gridded satellite estimates, gridded temperature observations, area of study, statistical methods. The results are described in Section 3 which contains spatial patterns of Rainfall onset, cessation, and Length of rainy season from the different techniques and thresholds. A discussion is presented in Section 4 and conclusions in Section 5.

2 Materials and methods

2.1 Study area

The study area covers the Intergovernmental Authority on Development (IGAD) member states of Sudan, Eritrea, Djibouti, South Sudan, Ethiopia, Kenya, Somalia and Uganda (Fig. 1). The region is characterized by complex topography, armed conflicts, and food insecurity. The region's elevation varies from an area below sea level over Sudan to the highest points of Mount Kenya at 5199 m as the second highest mountain in Africa after Mount Kilimanjaro (5895 m) in Tanzania. The IGAD regional climate is affected severely by the seasonal movement of intertropical convergence zone (ITCZ) north and southward which is one of the factors determining the variation in four different rainfall seasons such as December, January, February (DJF), March, April, May (MAM), June, July, August, September and October, November, December (OND). Also, many studies show the climate of region influenced by El Nino/Southern Oscillation (Ogallo, 1988; Indeje et al. 2000; Anyah and Semazzi, 2006; Otieno and Anyah, 2012) as well as variability of sea-surface temperature over the Indian Ocean (Williams and Funk, 2011). The impacts of different ENSO phases (El Niño and La Niña or neutral) have different impacts over different parts of the region (Clark et al. 2003; Otieno and Anyah, 2012). The variation in climatic zones whether warm deserts

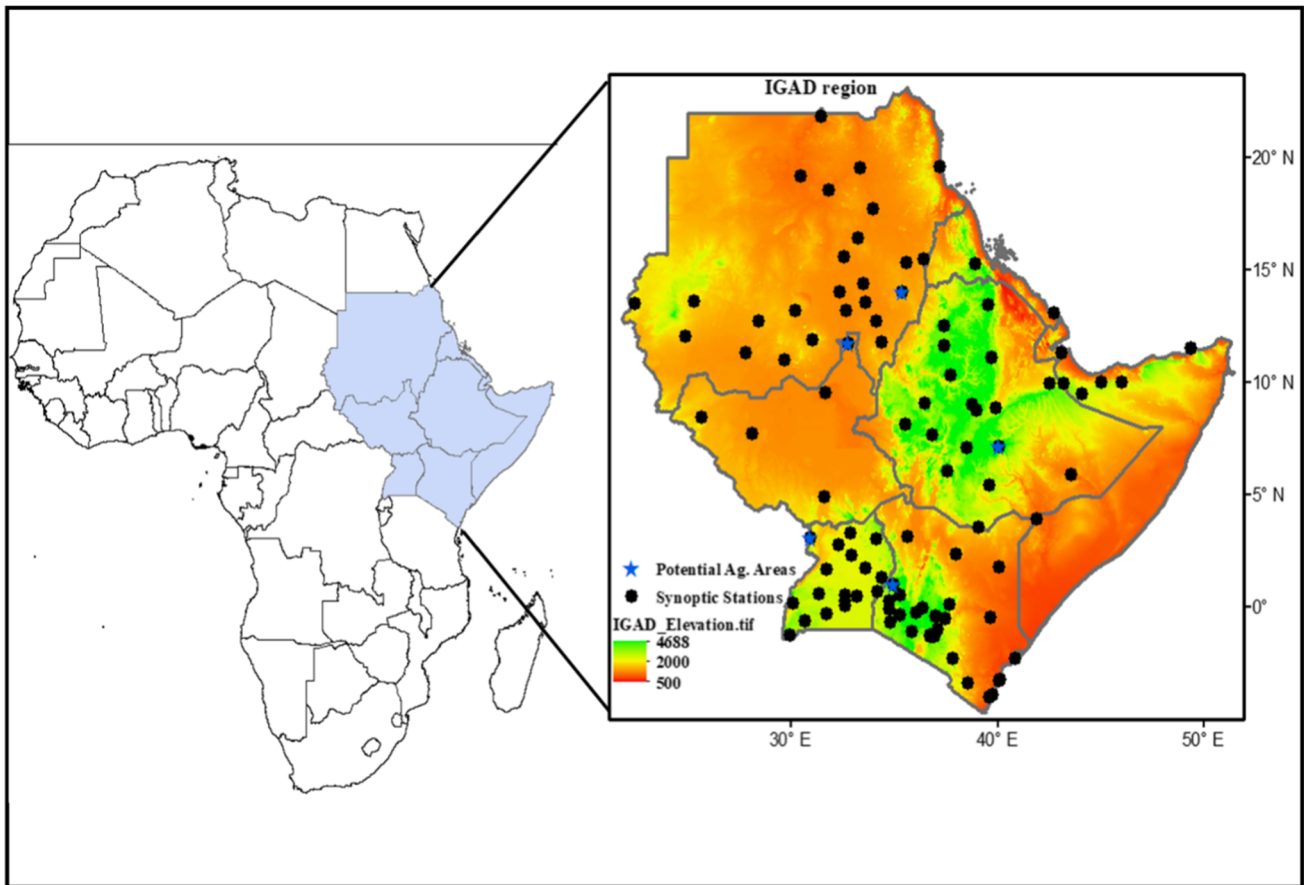


Fig. 1 Elevation map of the IGAD region of Eastern Africa showing the location of rain gauges stations (*) and five potential agricultural areas (*) used for evaluation temporal characteristics of RODs, RCDs and LRS from 1981 to 2021

or humid highland climate are mainly driven by orography, topography, and micro-synoptic systems (Peel et al. 2007).

2.2 Datasets

High-resolution Satellite Rainfall Estimates (SRE) products selected for this study are Climate Hazards Group Infrared Precipitation with in situ station (CHIRPSv2.0) daily datasets from the University of California at Santa Barbara (UCSB). CHIRPS product is developed at 0.05° spatial resolution, daily, pentadal, dekadal, and monthly temporal resolution and available from 1981 to near present (Funk et al. 2015). The multiple steps detailed major input datasets and processes, merging with station data, weighted bias ratios, homogeneity of the time series and algorithm used to generate CHIRPS products found in data documentation provided by Funk et al. (2015). The major steps for development of products are infrared precipitation (IRP) pentad (5 days) extracted from Globally Gridded Satellite (GriSat) and NOAA Climate Prediction Center dataset (CPC TIR) using cold cloud durations (CCDs) and calibrated using the Tropical Rainfall Measuring Mission Multi-Satellite

Precipitation Analysis (TMPA 3B42), in the second step, the percent of normal IRP pentad multiplied by the corresponding Climate Hazards Precipitation Climatology (CHP-Clim) pentad to produce an unbiased gridded estimate. In the third step, the final product of CHIRPS has been produced through merging stations with the CHIRP datasets. Although, CHIRPSv2.0 daily products are known to have errors in estimation of variance compared to dekadal and monthly products; however, the products still perform well in estimating intra-seasonal rainfall characteristics over East Africa. Also, validation at regional and national levels shows CHIRPSv2.0 has better performance compared to ARC2 and TAMSAT3 at dekadal and monthly, while TAMSAT3 better at daily (Dinku et al. 2018). In addition, use of daily products informed by results of validation of dekadal timescale, where the CHIRPSv2.0 validated against 104 synoptic station over IGAD region, TAMSAT v3.1, PERSIANN-CDR, CPC ARC2, CPC RFEv2, TRMM 3B42RT v7, CMORPH v1.0 CRT, GPM L3 IMERG v06 at dekadal time scale. The products found to have a few missing data, time scale going back to 1981, with only lag 2 days from last pentad, dekadal, and months compared to other products. Furthermore, the

quality of supported by hundreds of synoptics stations over east Africa region used in the merging with CHIRP raw products. The second datasets used in this study are the maximum and minimum temperature gridded datasets obtained from the NOAA Climate Prediction Center (CPC) at 0.5° resolution. The documentation of this data found at [NOAA NCEP CPC GTS GLOBAL gridded temperature daily \(columbia.edu\)](https://www.columbia.edu/~c115/NOAA_NCEP_CPC_GTS_GLOBAL_gridded_temperature_daily/). The water balance (WB) and evapotranspiration (PET), which used in calculating the RODs was derived from maximum and minimum temperature datasets re-scaled to CHIRPS resolution (0.5° grid) using bilinear interpolation method (Hietarinta, 2005).

2.3 Statistical methods and thresholds for rainfall, cessation, and length of season

There are a considerable number of definitions and thresholds for calculating rainfall onset and cessation dates patterns in the literature. In most cases, these definitions produce different RODs patterns and trends even when applied to the same observation or gridded dataset (e.g., Laux et al. 2008). The first and most used methods in literature are those apply threshold values on Total rainfall amount (e.g. (Stern et al. 1981, Sivakumar 1988, Segele and Lamb 2005, Marteau et al 2009, Marteau et al 2011), fraction of evapotranspiration, Walter method (Olatunde and Love, 2018)), Number of rainy days and spell lengths (Gudoshava et al. 2020b). All these methods observed limitation regarding

number of rainy days within threshold of total rainfall amount. Therefore, in this study, RODs, RCDs, LRS criterion and thresholds were determined by adopting combination of thresholds of rainy day, accumulated or total rainfall, number of rainy days and wet/dry spells lengths. The day considered to be rainy if observed at least 1 mm, the accumulated rainfall total of 20 mm over 5 days with at least 3 rain days and dry spell not exceeding 7 days in the next 21 days as described in (Table 1). The adoption of ROD criteria used in this study informed by nature of rainfall amount required for food crops such as maize and sorghum and humid climate in potential agricultural areas. In addition, to avoid early and unreasonable onset and cessation dates. The adoption of 5 days with at least 3 rain days and dry spells thresholds to give comprehensive assessment of accurate RODs patterns compared to what in the literature. Also, to capture accurate and reliable onset dates which is the main factor in the determination of LRS.

The RCD criterion and threshold that was applied in this study are the potential evapotranspiration and Water Balance criterion and threshold (Table 2). Potential Evapotranspiration (PET) derived from CHIRPS, maximum and minimum datasets using the Modified Hargreaves method (Cobaner et al. 2017). Then PET used to compute Water Balance (WB). The thresholds for WB are Soil Water Holding Capacity (SWHC) to be 100%. The datasets for each year computed separately from 1st January 1981 to December 2021. Then RCD computed

Table 1 Rainfall onset dates (ROD) criterion and thresholds

Onset dates criterion and threshold based on: number of rainy days and spell lengths
 Threshold for rainy day: 1 mm
 Rainfall total should be: 20 mm over 5 days with at least 3 rain days
 Dry spell not exceeding: 7 days in the next 21 days
 For MAM season earliest onset dates is 1st March and latest possible date is 31 May
 For JJA season earliest onset dates is 1st June and latest possible date is 31 August
 For SON season earliest onset dates is 1st June and latest possible date is 30 November
 For DJF season earliest onset dates is 1st December and latest possible date is 27 February

Table 2 Rainfall cessation dates (RCD) criterion and thresholds

Cessation dates criterion and threshold based on: fraction of evapotranspiration
 Threshold for rainy day: 1 mm
 Cessation method: fraction of evapotranspiration
 Detection: fraction of evapotranspiration
 Accumulated 10 days rainfall less than 0.5 of the evapotranspiration
 For MAM season earliest cessation dates is 1st April and latest possible date is 30 June
 For JJA season earliest cessation dates is 1st June and latest possible date is 31 August
 For SON season earliest cessation dates is 1st September and latest possible date is 30 November
 For DJF season earliest cessation dates is 1st December and latest possible date is 27 February

based on fraction of evapotranspiration and threshold used are accumulated 10 days rainfall less than 0.5 of evapotranspiration.

The statistical methods used to compute climatology baseline or mean state, variability, late/early and changes in ROD, RCD, and LRS are average of 30 years (1981–2010) for mean state (climatology) and baseline for coefficient of variation (CV) as recommended by World Meteorological Organization (WMO). To assess the changes in mean and variability of RODs, RCDs and LRS, the departure from the climatology for every decade (10 years) of 1981–1990, 1991–2000, 2001–2010 and 2011–2020, average of 40 years (1981–2020) and differences between current 20 years (2001–2020) and previous 20 years (1981–2000) are computed. The means state of each 10 years and current 20 years compared to previous 20 years (1981–2000) to determine the shift in dates backward (early onset and cessation) or shift in dates forward (late onset and delayed cessation), then to find out whether LRS become longer (increased in days) or shorter (decreased in days) compared to baseline period. The mathematical formulas of mean (\bar{X}), CV and change (∇X) are described in Eqs. (1) to (3) below:

$$\bar{X} = \frac{1}{N} \sum_{i=1}^n X_i \tag{1}$$

Where \bar{X} = average (or arithmetic mean), n is the sample size, X_i = the value of each individual item in the data being averaged. Change in mean (X^-), as described in Eq. 2

$$\nabla \bar{X} = \frac{1}{N} \sum_{j=1}^n X_j - \sum_{i=1}^n X_i \tag{2}$$

Where (X_j) represent current 20 years (2001–2020) and (X_i) represented previous 20 years (1981–2000). The coefficient variation (CV) which is standard deviation ratio (σ_x) divided by mean \bar{X} as described in Eq. 3.

$$CV(\%) = \left(\frac{\sigma_x}{\bar{X}} \right) * 100 \tag{3}$$

Where σ_x is standard division (SD) computed from Eq. 4 below.

$$\sigma_x = \sqrt{\frac{1}{n} \sum_{i=1}^n (x_i - \bar{x})^2} \tag{4}$$

Linux-based Climate Data Operators (CDO) commands lines, R-statistical Package Climate Data Tool (CDT), and ArcGIS 10.4 were used in plotting and mapping spatial maps.

3 Results

3.1 Changes and variability in rainfall onset dates

The spatial patterns of mean state of RODs over eight IGAD member states in Eastern Africa are presented in Fig. 2. The mean RODs for MAM season show that the onset criteria met in March over areas in southwestern and progression of dates continued from the southwestern in March to northeastern areas in May. The earliest onset date occurred in the first week to fourth week of March over most parts of southern and central districts of Uganda, highlands of western and Nyanza regions in Kenya and south-western Ethiopia. The coastal counties, north-eastern and central counties in Kenya, southern and central parts of South Sudan, southern and central Somalia, central and north-eastern Ethiopia, north-eastern Uganda observed mean RODs in the first week to third week of April (Fig. 2a). By the first week of June to second week of July, most parts of South Sudan, Ethiopia, southern parts of Sudan and northern Uganda have fully met rainfall onset thresholds and criteria. With exception of highlands of western and Nyanza region in Kenya, most parts of Somalia and Kenya experiencing the dry conditions (dry season) during JJA season, therefore RODs criteria not established (Fig. 2b). Similarly, Djibouti, north-eastern Ethiopia, most parts of Eritrea and central Sudan observed the mean RODs in August. By the first week of October, there were no indicators of RODs activities in Djibouti, Eritrea, central and northern Sudan, north-eastern Ethiopia and north Somalia. However, the short rains onset dates predominate over most parts of Kenya, southeastern Ethiopia, southern Somalia by the second week of October (Fig. 2c). The DJF are dry months over Sudan, South Sudan, northwestern and central Ethiopia, Djibouti and Somali (Fig. 2d). Furthermore, the Lake Victoria basin shows continuation of rainfall onset throughout the MAM, JJA, SON, and DJF seasons. In other words, the rainfall total of 20 mm over 5 days with at least 3 rain days and dry spell not exceeding 7 days in the next 21 days criteria are met from March to November.

Figure 3 shows the spatial patterns of the mean state of variability in RODs patterns for MAM, JJA, and SON seasons. The results show that variability in RODs over the IGAD region varies within seasons and geographical locations, however, the variability is generally less than 40% across the four seasons (MAM, JJA and SON and DJF). The highest variability (20–30%) during MAM season was recorded over central, northeastern Ethiopia, southeastern South Sudan, scattered areas in central and coastal parts of Kenya (Fig. 3a). The highest variability ranges between 20–35% during JJA season recorded over

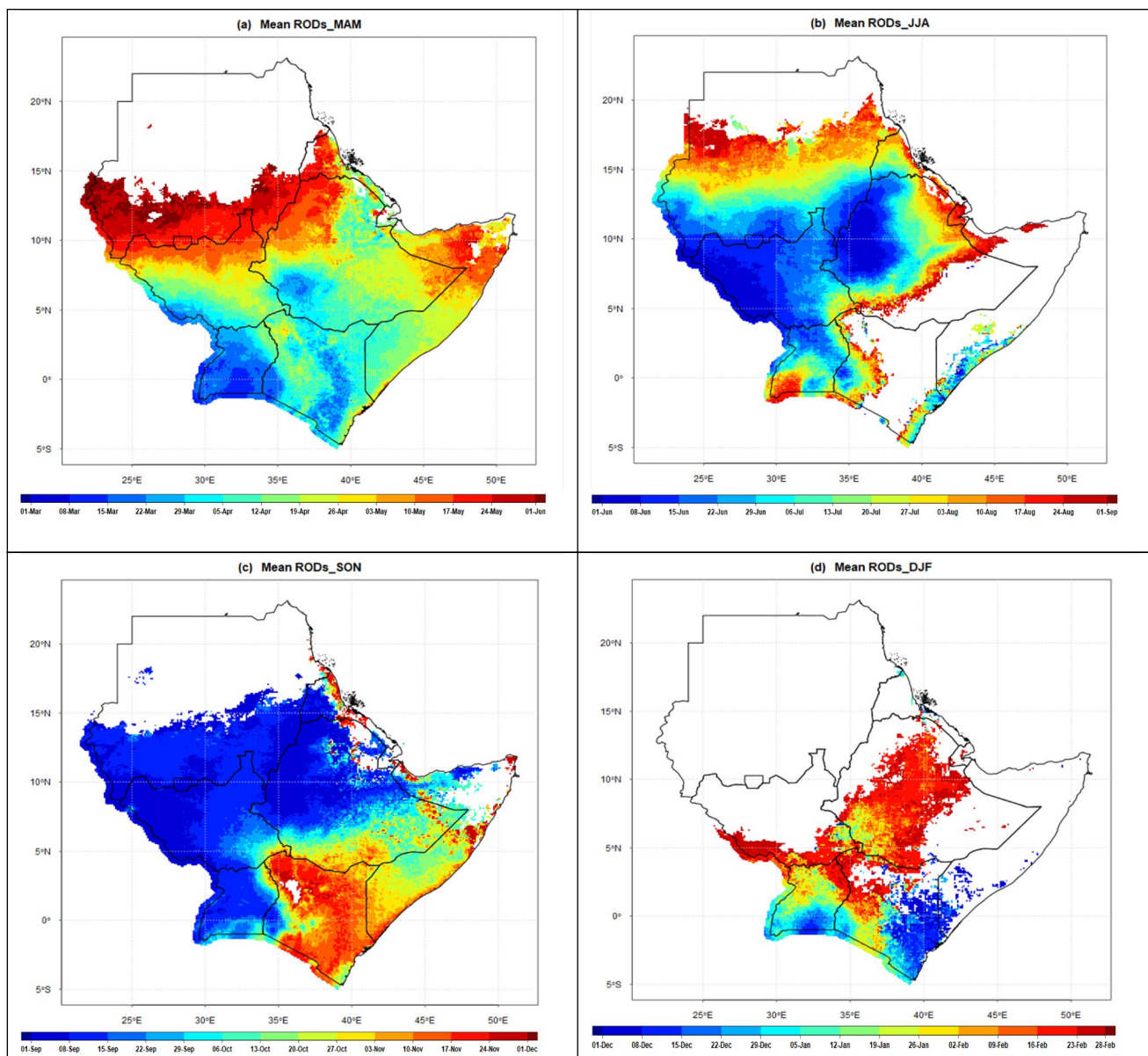


Fig. 2 Mean spatial patterns of rainfall onset dates (RODs) over IGAD region reference to (1981–2021) average during **a** MAM, **b** JJA, **c** SON and DJF. The pixel values presented as actual dates in standard calendar

southern and western districts in Uganda, highlands of western and Nyanza region in Kenya, southeastern South Sudan (Fig. 3b). Rift Valley in Kenya, Karamoja Region in northeastern Uganda, scattered areas in southern parts of Ethiopia recorded highest variability ranges between 20 and 30% (Fig. 3c). The DJF season recorded highest variability ranges between 24 and 35% over most parts of Uganda, Nyanza counties and southern parts of Kenya, southwestern Ethiopia (Fig. 3d). Western and southwestern parts of South Sudan, highlands of central and western Ethiopia zones recorded lowest variability ranges between 1 and 5% (Fig. 3b). Furthermore, SON season recorded

lowest variability ranges between 1 and 10% over most parts of South Sudan, southern parts of Sudan, Amhara zones in western Ethiopia. The DJF is dry season over most parts of the IGAD region; therefore, RODs variability criteria are not met over Sudan, Djibouti, Eritrea, Somalia, and ASALs in Kenya.

The changes in spatial patterns of mean RODs in last four decades (1981–1990, 1991–2000, 2001–2010, and 2011–2020), average of 40 years (1981–2020) and differences between current 20 years (2001–2020) and previous 20 years (1981–2000) compared to climatology (1981–2010) are presented in Fig. 4 (columns one to six respectively). The

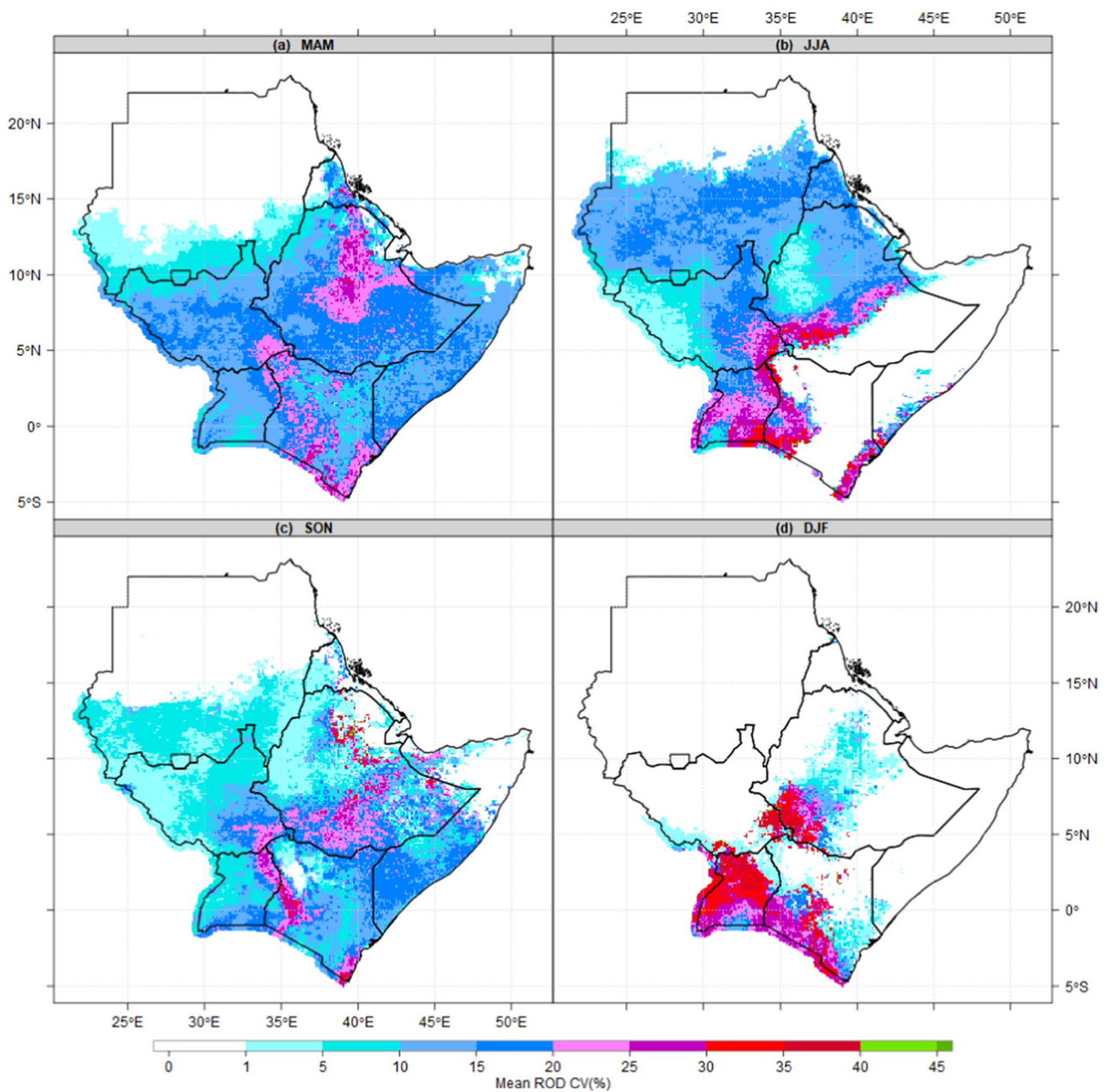


Fig. 3 Mean spatial patterns of variability in rainfall onset dates (RODs over IGAD region reference to (1981–2021) average during **a** MAM, **b** JJA, **c** SON and **d** DJF. The coefficient of variance (CV) val-

ues in the legend presented in percentage (%). The white and green areas represent the lowest and highest variability respectively

patterns are assessments of whether on average, a certain place is experiencing a delayed onset (positive values) represented with brown colors and early onset dates (negative values) in green colors. The results show a delayed 7–14 days (1–2 weeks) observed over most parts of South Sudan, Uganda, and Ethiopia in 1980s, southwestern South Sudan, central and western Kenya in 2010s during MAM season. JJA observed delay over South Sudan in northern Ethiopia and southern parts of Sudan in 1980s. Similarly, the delay

was observed over southern parts of Kenya, most parts of South Sudan, southeastern Sudan during SON. In the last decade (2011–2020), early ROD was observed over most parts of the IGAD region. The most observed early RODs during MAM season are southern and central South Sudan, southeastern Ethiopia, districts in central Somalia and southern Uganda during MAM (Fig. 4a–f) and JJA season(g–j). The SON season, observed 7–14 days early RODs over central Equatoria and Jonglei states in South Sudan, southern

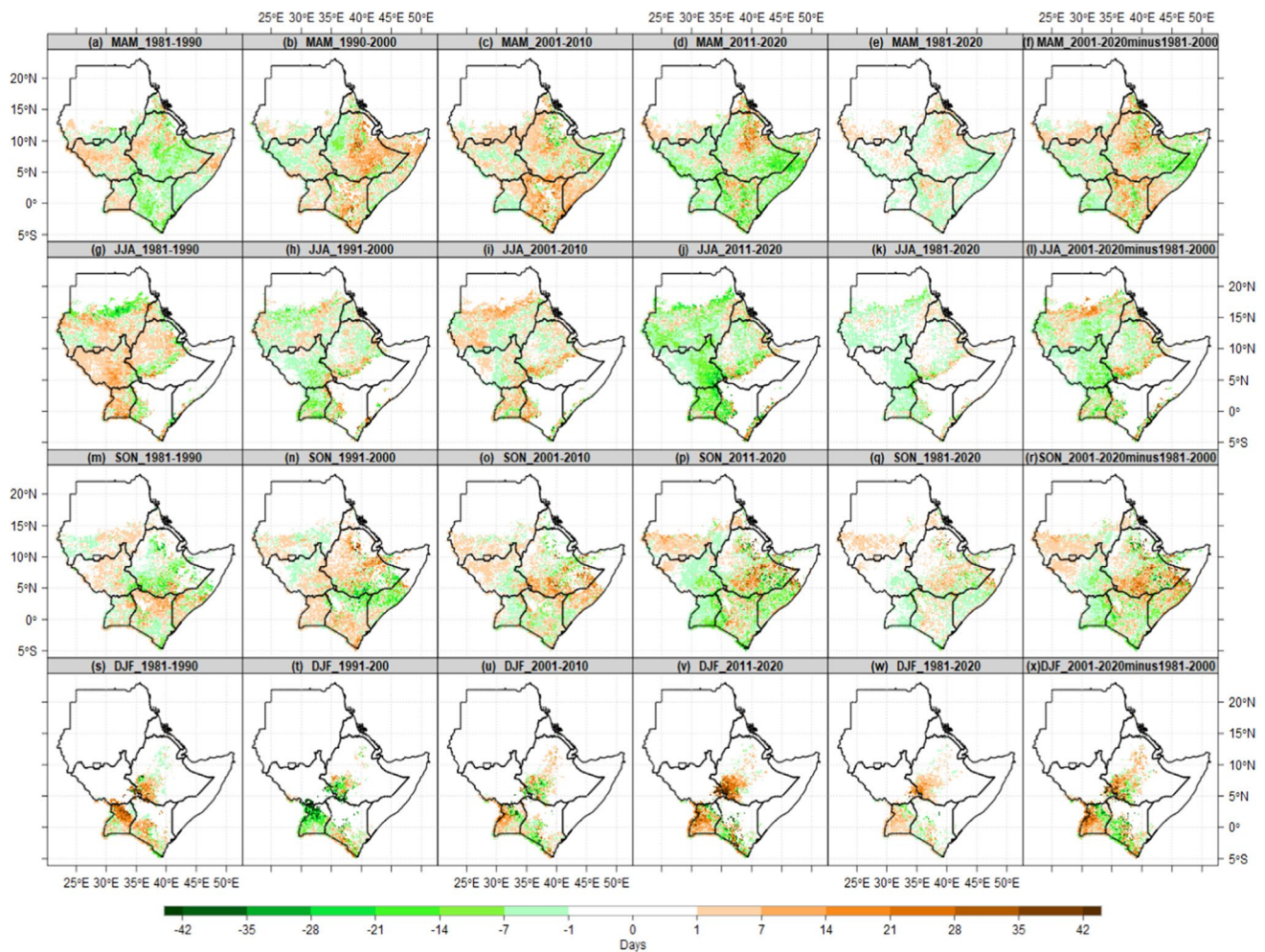


Fig. 4 Changes in RODs anomalies four decades (1981–1990, 1991–2000, 2001–2010, and 2011–2020), average of 40 years (1981–2020) and differences between current 20 years (2001–2020) and previous

20 years (1981–2000) relative to 1981–2010 reference period. The green color (negative values) indicates early RODs, while brown color (positive values) indicates delayed RODs

and central Uganda, highlands of western Kenya, southern Somalia (Fig. 4m–r). The criteria of RODs are not met over Sudan, Eritrea, Djibouti, Somalia, northern and eastern Ethiopia, South Sudan, and semi-arid counties in northeastern and northern Kenya during DJF season (Fig. 4s–x). Although there are opposite signals (delayed and early) onset dates in 1980s, 1990s, and 2000s compared to 2010s, the early RODs dominated the average patterns of all 40 years (1981–2020) over most parts of Kenya, southeastern Ethiopia, central Somalia during MAM season (Fig. 4d), and most parts of Uganda, and highlands of western Kenya and southern parts of South Sudan during JJA and SON (Fig. 4j, P).

The changes in spatial patterns of mean variability in RODs during the past four decades are presented in Fig. 5a–x. The areas with an increase in variability (positive values) in brown colors and decreasing in onset dates (negative values) in green colors. Generally, the increase (decreased) in RODs variability not exceeding 10% over the

region. The results show an increase in RODs variability observed in the 1980s over most parts of South Sudan, Ethiopia, southern and central Uganda during MAM (Fig. 5a–f), most parts of South Sudan, southern parts of Sudan during JJA season (Fig. 5g–l). The SON short rain recorded an increase in variability over northeastern Kenya, southern Somalia, southwestern Ethiopia (Fig. 5m–r). No changes in variability during DJF season because most parts of IGAD region are dry climatology (Fig. 5s–x). In 1990 to late 2000s, the decrease in variability was observed over most parts of the region during MAM and JJA seasons. Comparing departure of patterns of 1981–1990, 1990s, 2000s from climatology, the increase (5–10%) variability in RODs is observed over most parts of Ethiopia, southern parts of Uganda, and decreases over most parts of Kenya, northern Uganda and southern Somalia during MAM rainy season (Fig. 5a–f). The JJA season recorded widespread decrease in RODs variability over most parts of South Sudan, central Sudan,

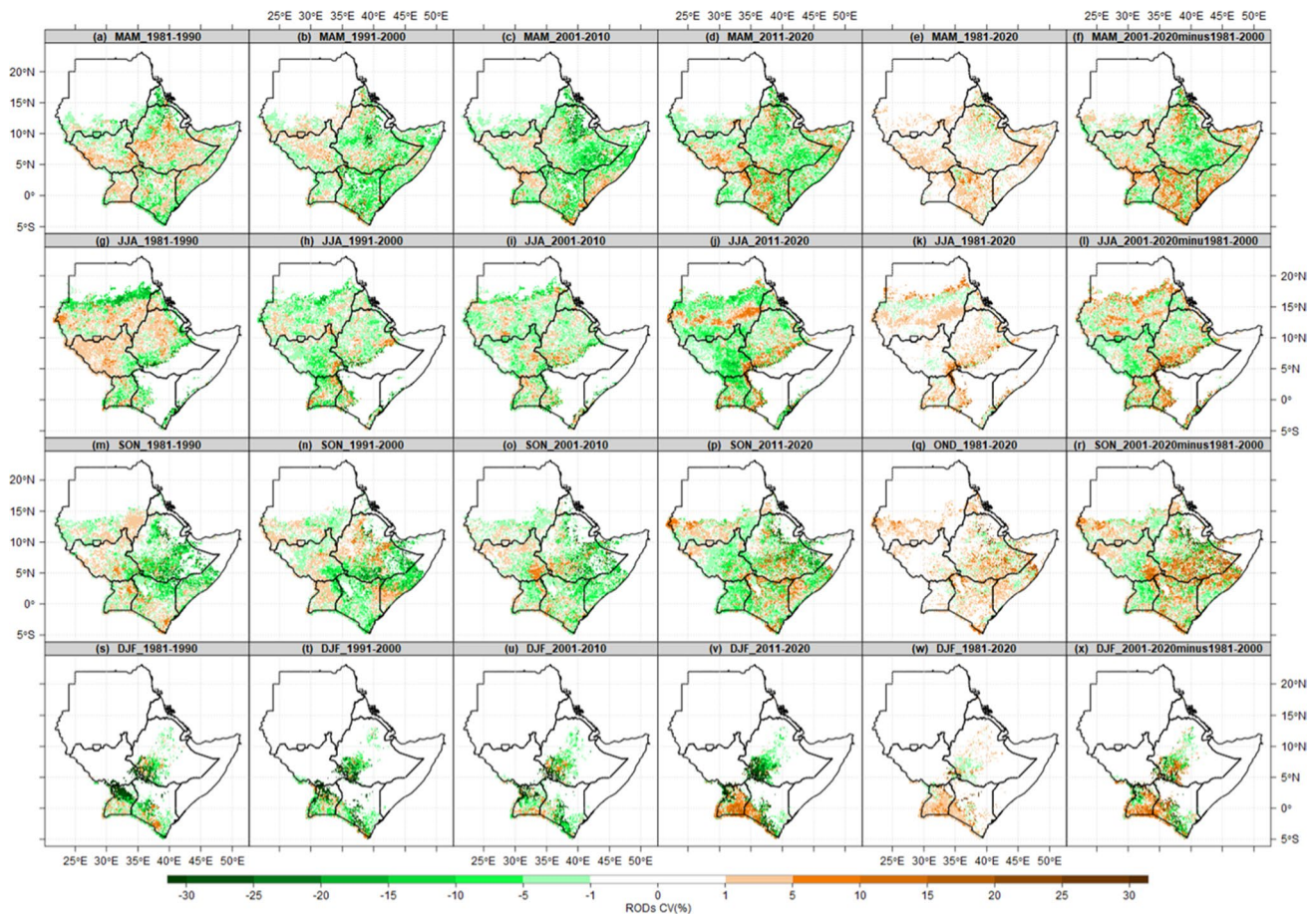


Fig. 5 Changes in variability of RODs anomalies of four decades (1981–1990, 1991–2000, 2001–2010, and 2011–2020), average of 40 years (1981–2020) and differences between current 20 years (2001–2020) and previous 20 years (1981–2000) relative to 1981–2010 ref-

erence period. The green color (negative values) indicates decreasing in RODs, while brown color (positive values) indicates increasing in RODs

highlands of central and northern Ethiopia, while southwestern Ethiopia observed increase ($< 5\%$) in variability (Fig. 10g–i). The last decade (2011–2020) observed lowest variability in RODs, therefore the trend of rainfall shows recovery and more wet conditions. The 5–20% decrease in variability observed in 2011–2020 and increase in variability ranges between 5 and 15% in early 1980s across all MAM, JJA, SON, and DJF seasons. These patterns neutralized the changes and reduced variability in RODs to less than 5% on average of 1981–2020 (Fig. 5e–w).

Figure 6a–d illustrates the spatial pattern of MAM, JJA, SON, and DJF mean RCDs, and the results revealed that the earliest mean cessation dates for MAM season occurred from 26 April, 3rd May, and 17 May over lower eastern and northern Kenya, southeastern Ethiopia and most parts of Somalia respectively (Fig. 6a). The JJA season showed mean cessation occurred from 1st June over southern, northeastern and northern Kenya, central and northern Somalia as confirmation of perceived dry season over most parts of Kenya and

Somalia. Similarly, the rainy season, which starts from June and July over northern sector of IGAD region, shows signs of cessation from 3rd August over central Sudan, northeastern Ethiopia, western Eritrea and Djibouti. In addition, no cessation criteria met as rainfall of the boreal summer continued over South Sudan, central and northern Ethiopia. The long rain continued over highlands of western Kenya, most parts of Uganda up to the end of November (Fig. 6b). The arid and semi-arid (ASALs) areas in Kenya, central Somalia, south-eastern Ethiopia already experienced rainfall cessation by 10 June as the beginning of dry season which continues to end of September. However, SON season shows the ceased rainfall patterns over most parts of Kenya and Somalia, southeastern Ethiopia started again in October and continued to end of November (Fig. 6c). The cessation occurred fully from 1st of December over most parts of region during DJF with exception of Lake Victoria basin sides in Kenya and Uganda and southwestern Ethiopia, while rainy season continued up to 5th of January over highlands of western,

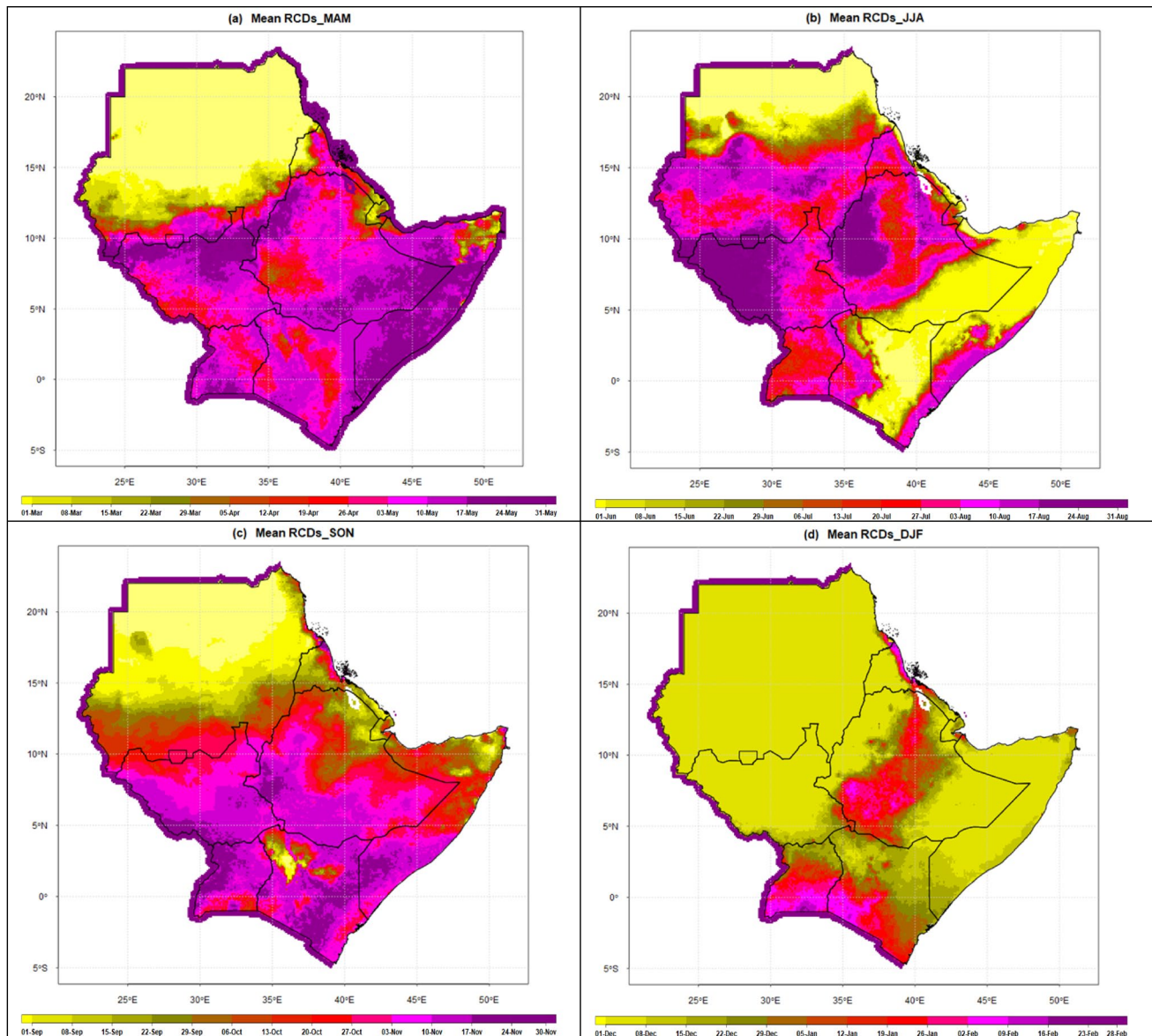


Fig. 6 Mean spatial patterns of rainfall cessation dates (RCDs) over IGAD region reference to (1981–2021) average during **a** MAM, **b** JJA, **c** SON and **d** DJF. The pixel values presented in actual dates in standard calendar

Nyanza region in Kenya and southern parts of Uganda (Fig. 6d). Moreover, the dry conditions which occurred in DJF season over most parts of region continued in MAM, JJA, and SON seasons over extreme northern parts of Sudan. These patterns are not considered as cessation dates because these areas are dry climatology. Similarly, no significant signals of rainfall cessation occurred over highlands of western Kenya and Nyanza region, most parts of Uganda and Ethiopia during MAM, JJA, and SON seasons. These areas favored a conducive environment for rain-fed agriculture from March to November, unlike ASALs areas in Somalia, Kenya, southeastern, and northeastern Ethiopia, where food insecurity and drought emergencies are stories of days

exacerbated by initial conditions of long cessation of JJA and DJF rainfall over these areas (Fig. 6b, d).

3.2 Changes and variability in rainfall cessation dates

Figure 7a–d shows the spatial patterns of the mean state of variability in RCDs. It is observed that the highest RCDs variability values did not exceed 40–45% across all seasons. The highest variability observed over a squall line extended from south Darfour in the west to Al Qadaref state in eastern Sudan during MAM season. The RCD values ranges between 30 and 40% re observed over South Darfour, South

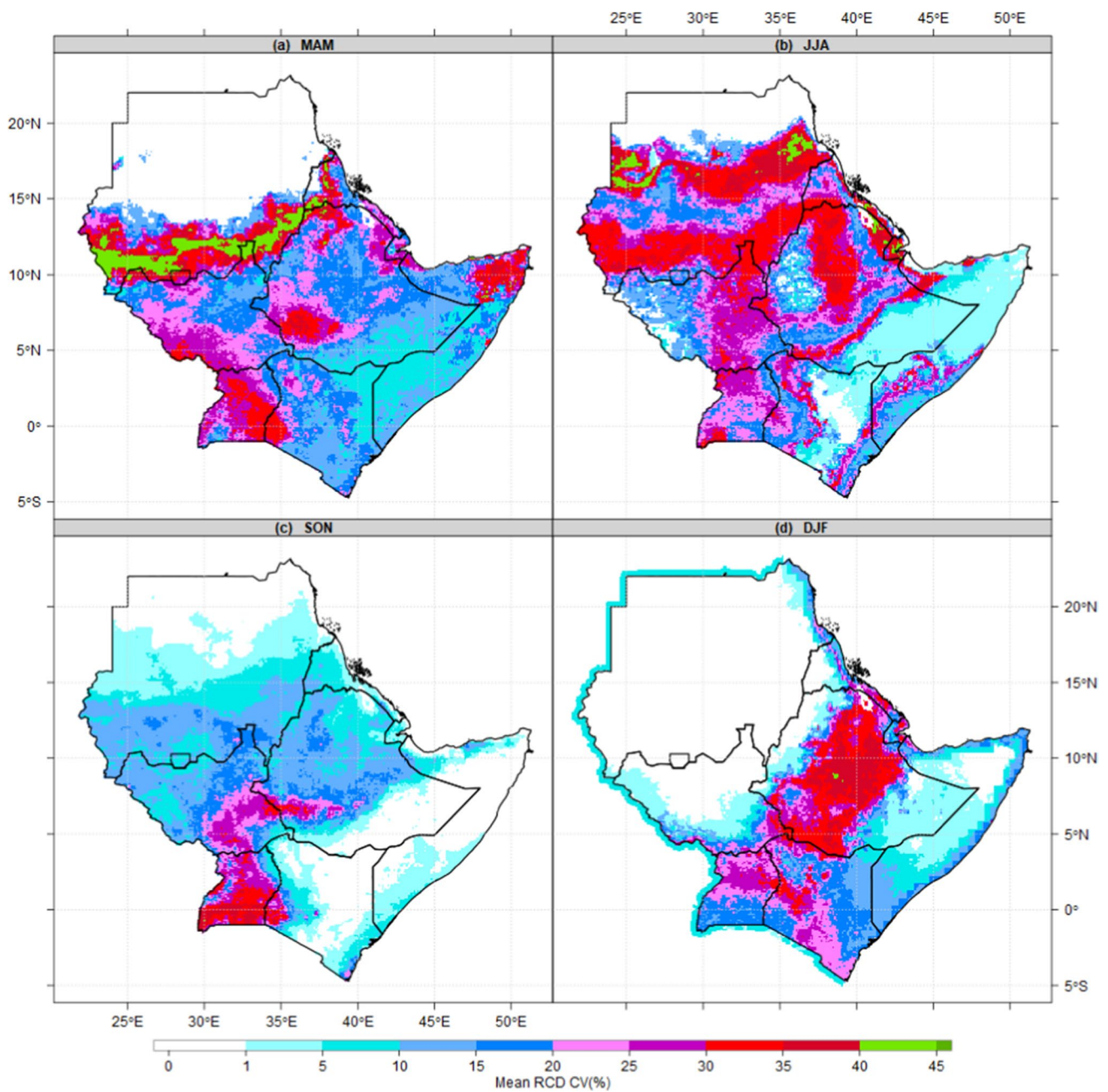


Fig. 7 Mean spatial patterns of variability in rainfall cessation dates (RCDs) over IGAD region reference to (1981–2021) average during **a** MAM, **b** JJA, **c** SON and **d** DJF. The coefficient of variance (CV) val-

ues in the legend presented in percentage (%). The white and green areas represent the lowest and highest variability respectively

Kordofan, White Nile state, coastal parts of Red sea in Sudan and Eritrea, and northeastern Upper Nile South Sudan. Similar patterns of variability observed over Tigray and Wollo zones in northern and central Ethiopia during JJA (Fig. 7b). In addition, districts in central and southern Uganda, and Nyanza region in Kenya observed highest variability during SON season (Fig. 7c), while central and northeastern zones in Ethiopia observed highest variability during DJF season (Fig. 7d). Furthermore, lowest variability observed ASALS

in Sudan, Kenya, Somalia, and southeastern Ethiopia. It is observed that the region with the highest total rainfall amount observed highest values of variability in RCD, while low variability in RCD observed in areas receiving less rainfall on annual and seasonal timescale over the IGAD region.

Figure 8 shows the spatial patterns of changes in mean RCDs. The changes or shifts in RCDs are assessed by comparing the four decades (1980s, 1990s, 2000s, and 2011s), average of 40 years and current 20 years (2001–2020)

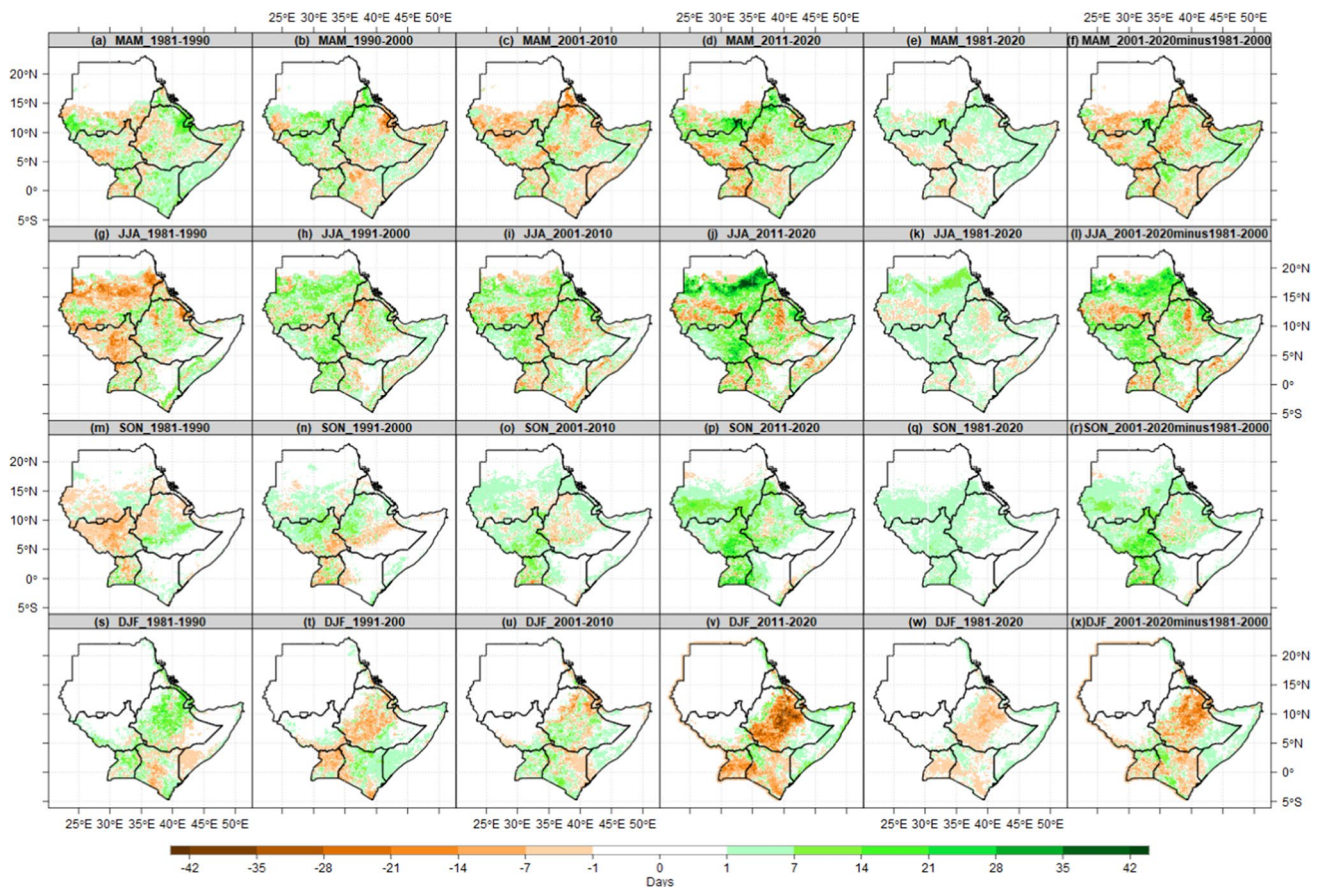


Fig. 8 Changes in RCDs anomalies of each four decades (1981–1990, 1991–2000, 2001–2010, and 2011–2020), average of 40 years (1981–2020) and differences between current 20 years (2001–2020) and pre-

vious 20 years (1981–2000) relative to 1981–2010 reference period. The brown color (negative values) indicates early RCDs, while green color (positive values) indicates delayed RCDs

compared with the past 20 years (1981–2000). The brown color (negative values) indicates early RCDs, while green color (positive values) indicates delayed RCDs. The recent years (2011–2020) show delay of 7–14 days in mean cessation dates over northeastern South Sudan, northwestern Kenya, western Sudan, sporadic parts in northern Somalia, and central and northwestern Ethiopia (Fig. 8 a–f). The JJA season experienced 7–21 days delayed cessation dates over central parts in Sudan, both northern South Sudan and Uganda, and northeastern Ethiopia (Fig. 8g–l). Similarly, the SON season experienced 14–21 days delayed RCD over most parts of South Sudan and Sudan (Fig. 8m–r). The early RCD over most parts of Sudan and South Sudan in the 1980s during JJA and SON. The recent years 2011–2020 observed early RCDs observed over most parts of Kenya, Ethiopia, and Uganda during DJF season (Fig. 8v, x)

The changes in variability of RCDs during the MAM, JJA, SON, and DJF seasons show high variability during MAM and JJA compared to SON season. The region experienced fluctuations of variability signals from decade to decade. For example, northern parts of South Sudan observed

decreases in 1980s and 1990s, while the signals turned to opposite in 2000s and 2020s. The 2000s and current decade (2011–2020) observed an increase in variability over most parts of Uganda, Ethiopia, and South Sudan during MAM (Fig. 9c, d). South Sudan is the most country observed the highest decrease in variability of RCDs (between 5 and 15%) during JJA season in 2000s and 2010s (Fig. 9i, j). Most parts of Sudan observed increased variability in 1990s during SON (Fig. 9n), most parts of Kenya in 1990s during DJF (Fig. 9t). With the exception of northwestern South Sudan, the average of 40 years showed increased variability over most parts of the region (Fig. 9e–w). Most parts of Kenya in 1980s, northern Uganda 1990s observed decreased variability during DJF season.

3.3 Changes and variability in length of rainy season

Figure 10 presents the spatial patterns of mean LRS, which is the number of rainy days between onset and cessation. The results revealed that southern parts of Uganda, western parts

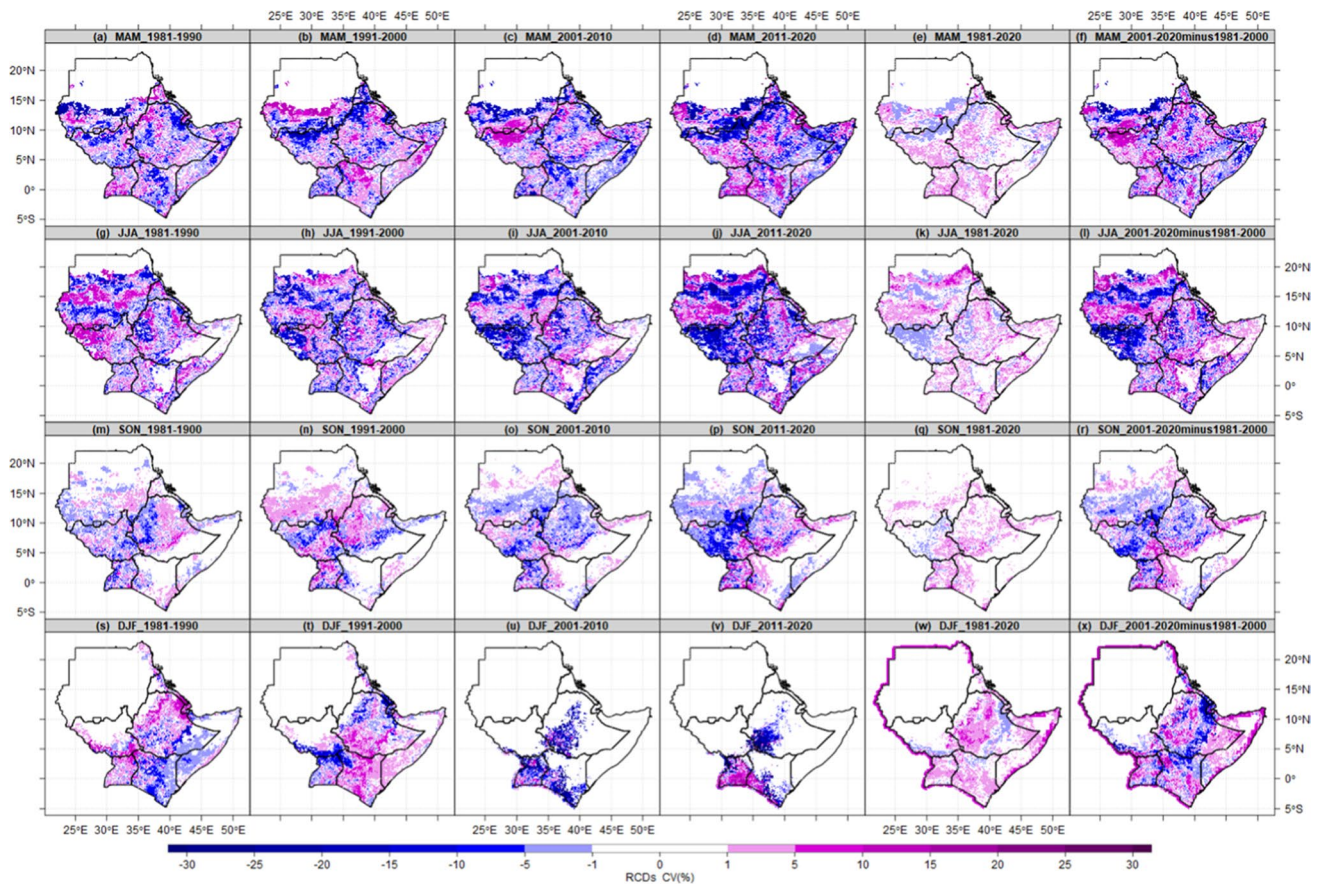


Fig. 9 Changes in variability of RCDs anomalies four decades (1981–1990, 1991–2000, 2001–2010, and 2011–2020), average of 40 years (1981–2020) and differences between current 20 years (2001–2020) and previous 20 years (1981–2000) relative to 1981–2010 reference

of South Sudan and highlands of western Ethiopia recorded the highest LRS (60–80 days), (80–90 days), (60–80 days) during MAM, JJA, and SON seasons respectively. Arid and semi-arid areas in Djibouti, Eritrea, northern Somalia, everywhere in Sudan, central and northern parts of South Sudan, and western and northern Ethiopia received LRS ranging between 1 and 20 days (Fig. 10a). The JJA, which is mainly rain-fed agriculture activities over South Sudan, Sudan, and Ethiopia with length of rainy days exceeding 80 days (Fig. 10b). Similarly, northern Uganda, highlands of western and Nyanza counties in Kenya, south-eastern and north-eastern parts of South Sudan, eastern and north-eastern Ethiopia, and southern parts of Sudan recorded rainy days ranging between 30 to 70 days during SON season (Fig. 10c). With the exception of districts in southern parts of Uganda, Nyanza Region, and coastal counties in Kenya, most parts of the region are dry during DJF season (Fig. 10d). On other hand, the determination of LRS failed over northern parts of Sudan during MAM, ASALs countries in Kenya, southeastern Ethiopia, and central and northern Somalia during JJA.

The blue color (negative values) indicates decreased variability, while purple color (positive values) indicates increased variability of RCDs

The unestablished RODs and LCDs patterns and nature of dry conditions (dry climatology) leads to unaccounted LRS.

The spatial patterns of mean state of variability in length of rainy season (LRS) presented in Fig. 11. The values of CV in the legend presented in percentage (%) with low (high) values mean low (high) variability. The results show high variability (> 30%) in LRS over most parts of Uganda, southern parts of South Sudan, western Kenya, and central Ethiopia during MAM season (Fig. 11a). The same patterns were observed again over Uganda, southern and northeastern South Sudan, and southern parts of Sudan during JJA (Fig. 11b). The high variability during SON observed over central and northern Uganda, south and southeastern South Sudan (Fig. 11c). Similarly, Oromia of zones in Ethiopia, districts in Uganda, western and southern parts of Kenya observed highest variability in LRS during DJF season (Fig. 11d). The lowest variability in LRS is observed over Sudan during MAM, Somalia, southern and northern Kenya during JJA, most parts of South Sudan, northern parts of Kenya, and everywhere in Somalia and Sudan during DJF.

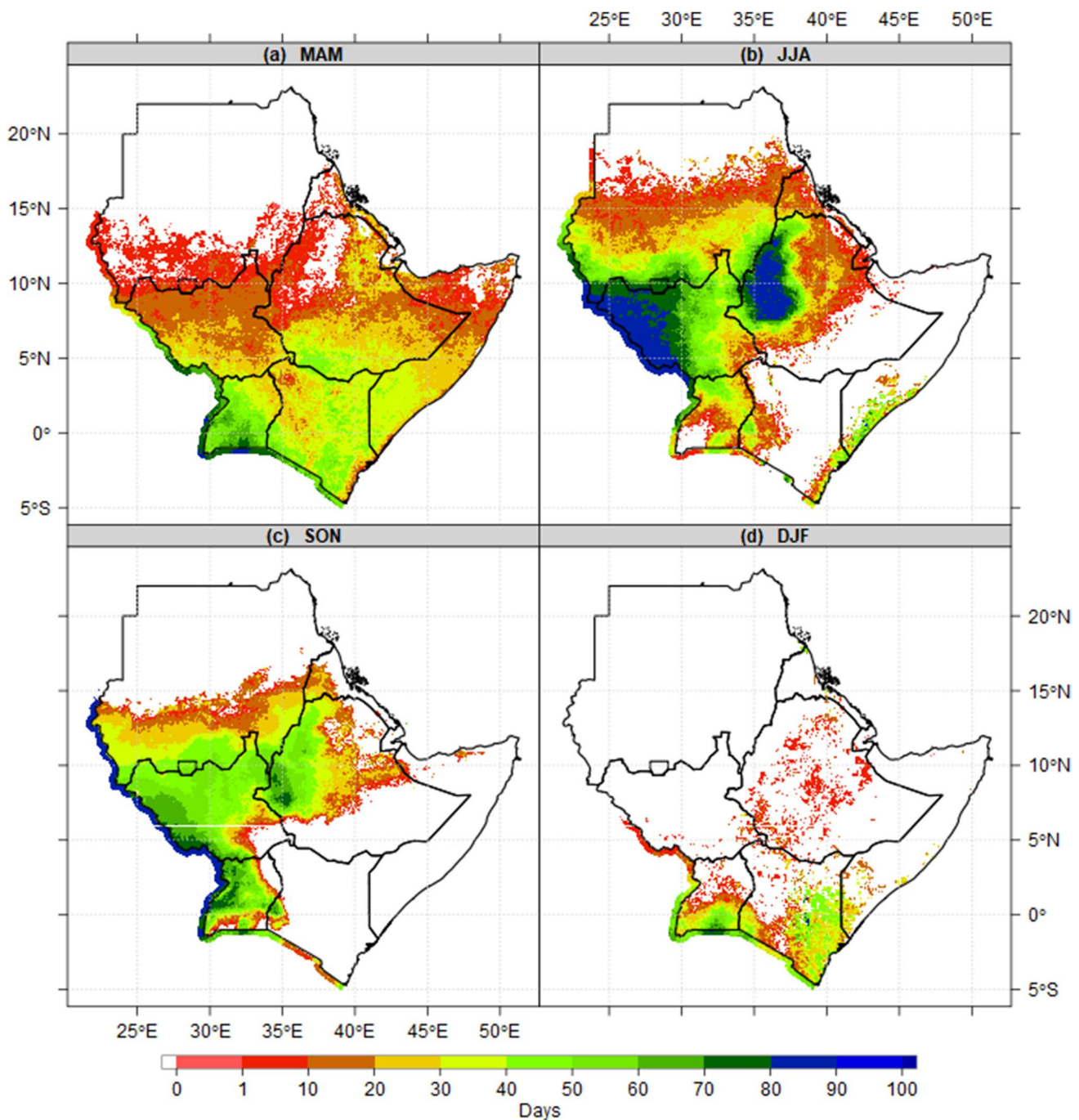


Fig. 10 Mean spatial patterns of length of rainy season (LRS) over IGAD region reference to (1981–2021) average during **a** MAM, **b** JJA, **c** SON and **d** DJF. The values in the legend presented in day

The results show clearly, the region with high rainfall intensity has lower LRS variability compared to arid and semi-arid. The patterns of variability in LRS not captured well over dry areas due to failed and inconsistent timing of rainfall onset and cessation dates.

Figure 12 presents the spatial patterns of changes in LRS on decadal and season time scale. The results show the recent 20 years (2001–2020) observed prolonged LRS

over southeastern Ethiopia, central Somalia, southwestern South Sudan, southwestern Uganda during MAM (Fig. 12f), most parts of South Sudan and Uganda during JJA and SON (Fig. 12l, r). The 2011–2020 decade is the most observed period 12–21 days increased (prolonged) in LRS over most parts of the IGAD region. Most parts of Kenya, central and southeastern Ethiopia observed 14–21 days of prolonged LRS in the 1980s. The 1980s decade

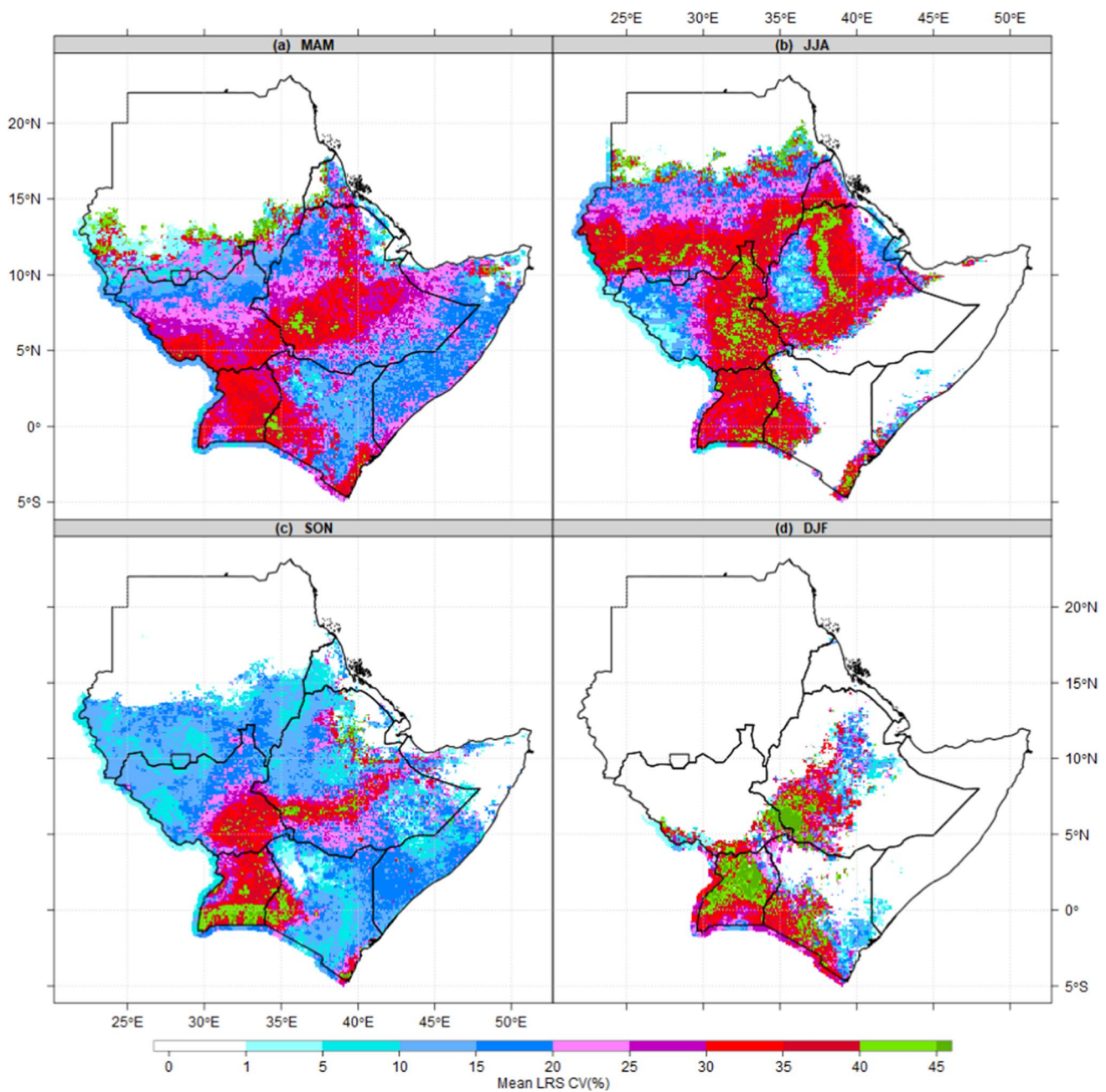


Fig. 11 Mean spatial patterns of variability in length of rainy season (LRS) over IGAD region reference to (1981–2021) average during **a** MAM, **b** JJA, **c** SON and **d** DJF. The values in the legend presented in percentage (%)

observed shortened (decrease of 7–14 days) in LRS over South Sudan during JJA and SON (Fig. 12g, m), while most parts of Kenya and Ethiopia observed shortened in 1990s and 2000s during MAM (Fig. 12b, c). Furthermore, the DJF season in recent decades (2011–2020) became very short with 14–28 days over most parts of Uganda, Ethiopia, and Kenya (Fig. 12s–x). The early ROD and delayed RCD played significant role in prolonged (increased) LRS over South Sudan and Uganda during JJA and SON in the 2011–2020 decade. Similarly, the delayed

ROD and early RCD are the main drivers of shortened LRS over most parts of the IGAD region in 1998s.

The change in the LRS variability for MAM, JJA, SON, and DJF seasons presented in Fig. 13. The highest decreased LRS variability of 10 to 20% observed in 2011–2020 decade (Fig. 13d–v). The highest increased variability was observed over western South Sudan and central Ethiopia in 1998s during MAM and JJA seasons (Fig. 13a, g). In addition, highlands of western Ethiopia, most parts of Uganda and southern Somalia observed increased variability in the

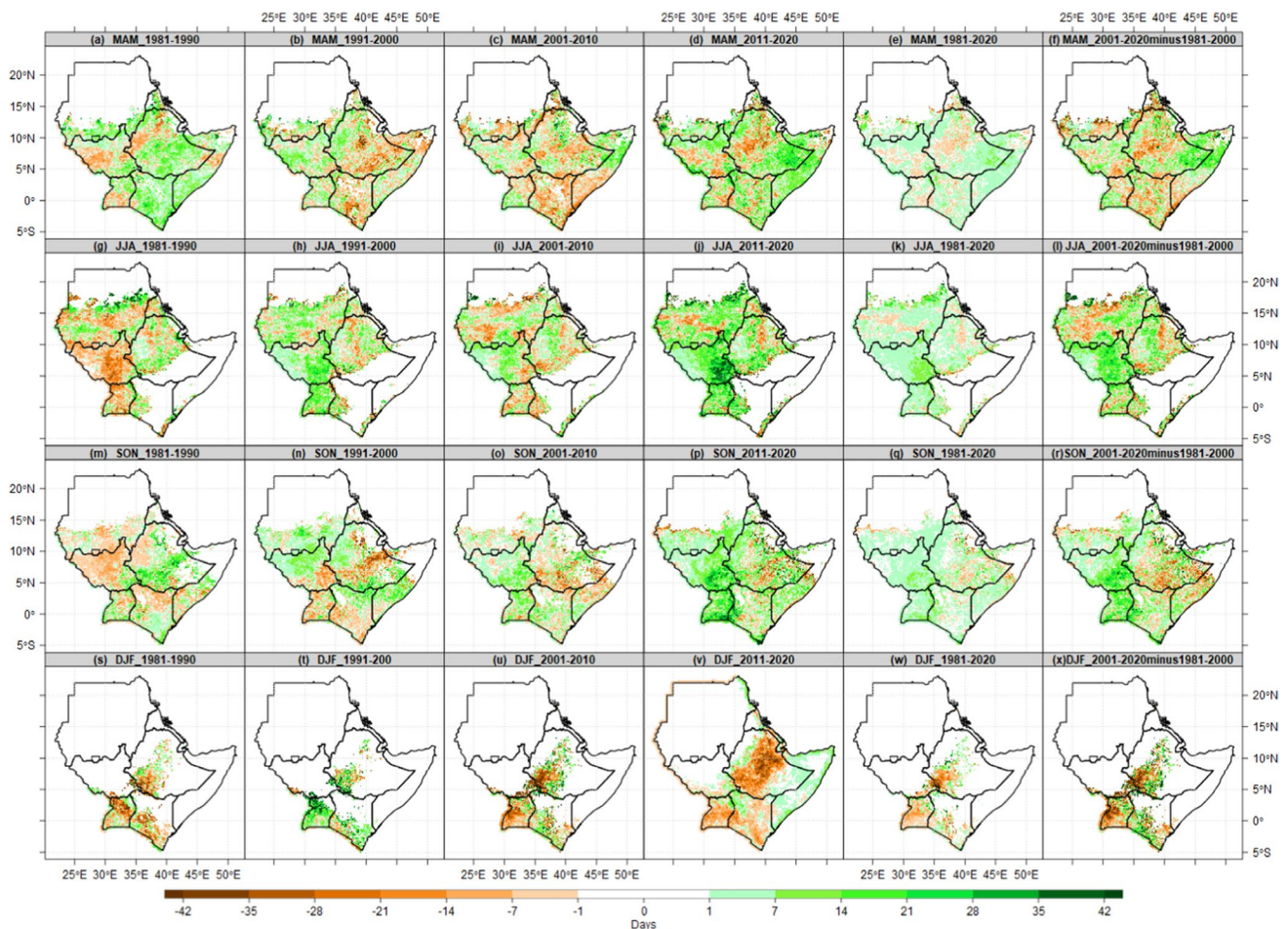


Fig. 12 Changes in LRS anomalies of four decades (1981–1990, 1991–2000, 2001–2010, and 2011–2020), average of 40 years (1981–2020) and differences between current 20 years (2011–2020) and pre-

vious 20 years (1981–2000) relative to 1981–2010 reference period. The cyan color (negative values) indicates decreased LRS, while brown color (positive values) indicates increased variability LRS

1990s during SON (Fig. 13n). An increase in variability of 10 to 20% experienced over southwestern Ethiopia, highland of western and central during SON season (Fig. 13m–r) and most parts of districts in Uganda during DJF season (Fig. 13s–x). The changes in LRS variability of current 20 years (2011–2020) compared to previous 20 years (1981–2000) shows the decrease of 5 to 20% in mean state of variability over eastern Amhara region, zones in Somali region of southeastern Ethiopia, and Mudug and Nugaal districts in Somalia during MAM (Fig. 13a–f). Similarly, a decreased variability of 5 to 20% experienced over northern and southwestern parts of South Sudan during JJA season (Fig. 13l). The average of variability in 40 years (1981–2020) stands at 1–5% due to lower variability in 2000s and 2011s compared to 1980s and 1990s (Fig. 13e–w). Comparing the patterns of variability in LRS with variability in ROD and RCDs, the decreased in LRS variability associated with early ROD, prolonged RCD, while increased variability coincided with late RODs, early cessation.

3.4 Implications of changes in rainfall onset and cessation dates on length of rainy season

This sub-section presents the implications of changes in RODs and RCDs on LRS. The patterns of changes in RODs, RCDs, and LRS at selected 54 districts in Sudan, 45 counties in South Sudan, 50 zones in Ethiopia, all 47 counties in Kenya, and 45 districts in Uganda presented in Fig. 14. The results show yearly cyclic variation in patterns of RODs, RCDs and LRS over the IGAD region. The changes in RODs and RCDs resulted in changes in LRS. The early mean RODs coincided with late mean RCDs resulting in shortened LRS if extended cessation dates longer than onset. This could be seen clearly in Khartoum in Sudan. The late RODs coincided with late RCDs resulting in prolonged LRS as in the case of Kutum in western Darfour in Sudan. On the other hand, the late RODs coincided with early cessation resulting in shortened LRS which is the dominant signal over most parts of IGAD region. Similarly, some regions observed

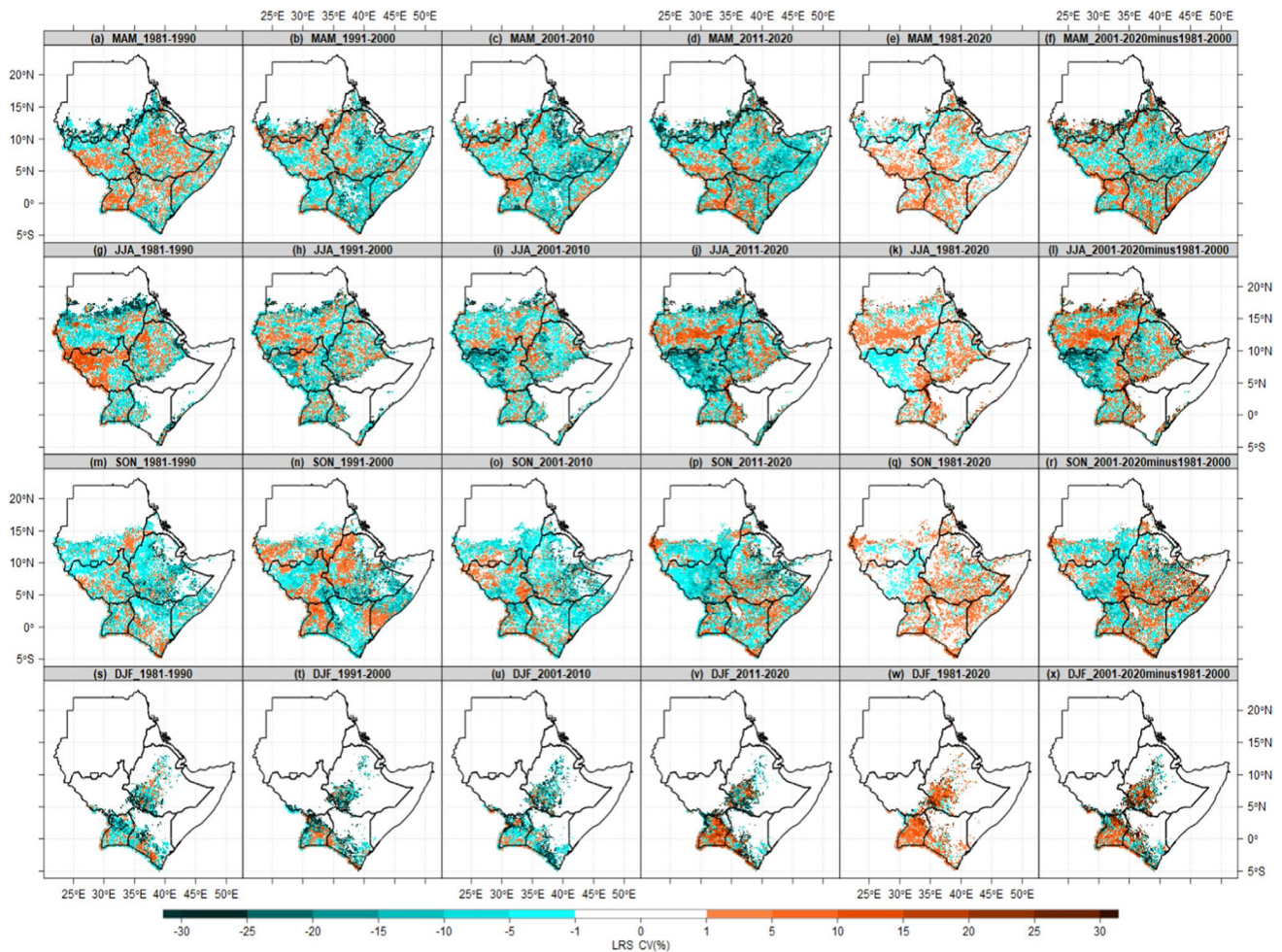


Fig. 13 Changes in variability of LRS anomalies of four decades (1981–1990, 1991–2000, 2001–2010, and 2011–2020), average of 40 years (1981–2020) and differences between current 20 years (2001–2020) and previous 20 years (1981–2000) relative to 1981–2010 ref-

erence period. The brown color (positive values) indicates increased variability, while cyan color (positive values) indicates decreased variability of LRS

late (delayed) RCDs lead to prolonged LRS. No significant impacts of early/late RODs on LRS, however, changes in RCDs have significant impacts on LRS (prolonged or shortened) over many areas in Sudan, South Sudan, Kenya, and Uganda. The nature of climate over ASALs in the region made it so difficult in some cases to differentiate between the real RCDs and the continuation of the dry season.

The inter-annual and decadal variability of RODs, RCDs and LRS in last 41 years (1981–2021) over five potential agricultural production areas in the IGAD region presented in Fig. 15. The results show the implication of changes in RODs and RCDs on LRS. These could be seen clearly in Arua District in Uganda, where The LRS shorten by 55 days in 2002 due to 66 days early cessation, 42 in 2008 due to 35 delayed onset and 7 days early cessation, 35 in 1983 due to 35-day delayed onset, 26 days in 2009 due to 24 delayed onset and 2 days early cessation, 22 days in 2021 due to 19

days delayed onset and 3 days early cessation. These patterns of change in LRS repeated over many areas in the region. No any signs on RCDs dates observed in 1997, 2012, and 2019 because of extra-ordinary rainfall continued from January to December. This happened simply due to accumulated 10 days rainfall less than 0.5 of the evapotranspiration thresholds for RCDs which established from January to December. The patterns of RCDs for Kitale in Kenya show that the season shorten by 129, 69, 66, 55, 52, 40 days in 2021, 2018, 2007, 1994, 2014, and 1983 respectively due to early cessation. Also, area observed 40, 43, 47, 59, and 69 days increase in LRS in 1995, 2019, 2016, 2017, and 1989 due to early RODs and delayed RCDs. For example, in 2021 as one driest year over East Africa, although the RODs started early by 9 days from the mean the RODs which is 13 April, however, the season shortened by 121 days (4 months) to 139 days early cessation. This situation simply mean RODs

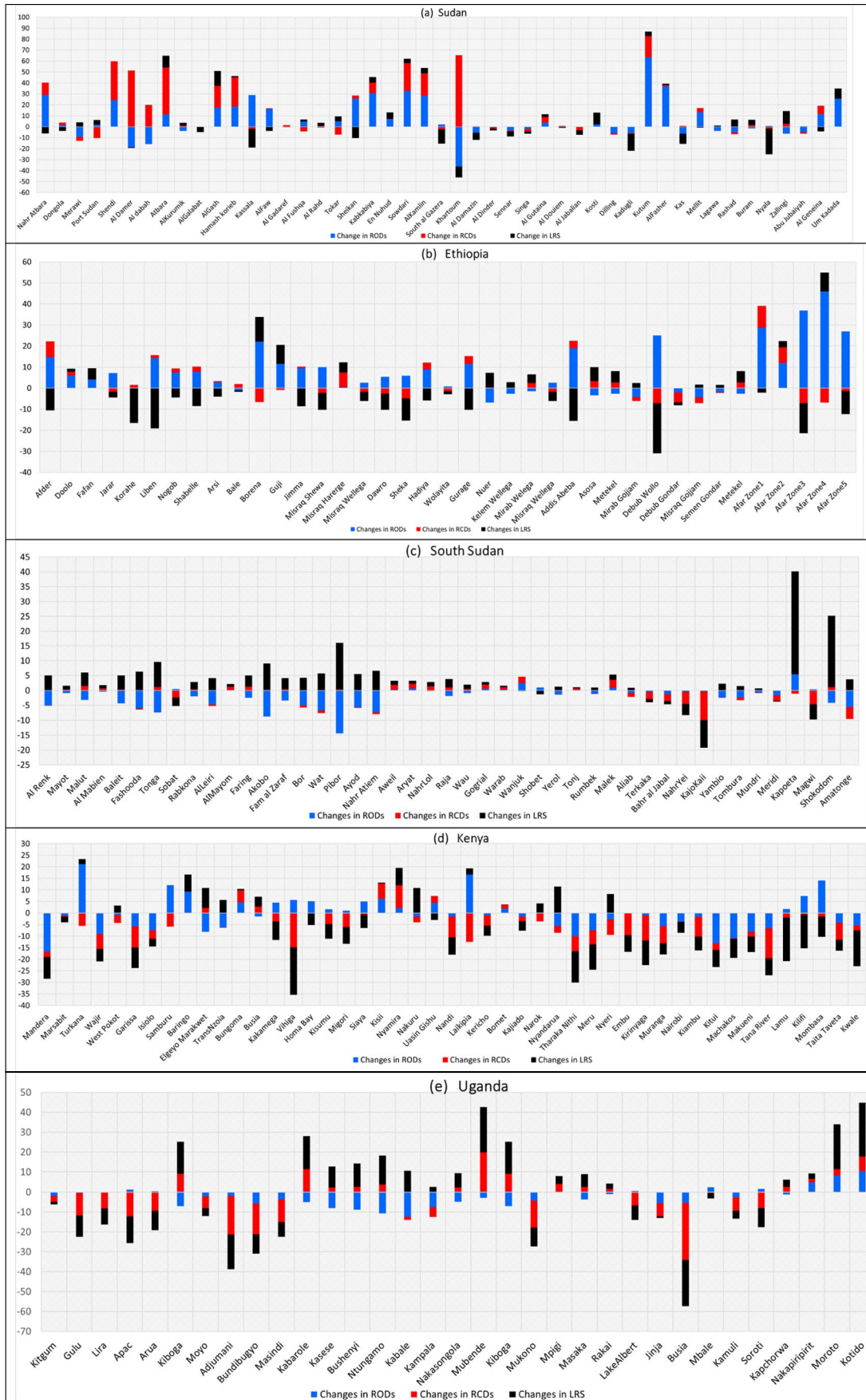


Fig. 14 The changes in RODs, RCDs, and LRS at selected countries local administrative levels: 48 districts in Sudan, 45 counties in South Sudan, 50 zones in Ethiopia, all 47 counties in Kenya, and 45 districts in Uganda

criteria met only in the first month then thresholds and criteria of RCDs established for next 4 months. These patterns derived by threshold of Soil Water holding capacity and unestablished accumulated 10 days rainfall less than 0.5 of the evapotranspiration threshold. Robe in Ethiopia, the failed RODs during MAM and JJA seasons in 1999, 2002, 2008, and 2016, leads to unclear LRS. Similarly, 118, 95, 62, 53, 32 days shorten LRS in 2021, 2011, 1995, 1989, and 2015 attributed to early cessation and late onset. Furthermore, the 48, 38, 35, 31 days early RODs in 2016, 2017, 1991, 1997, and 1993 over El renk in South Sudan, resulted in increased LRS, while late onset in 2020, 1981, 2000, 2015, 1982, and 1984 resulted in shorten of LRS by at least 18–34 days. The 71 days early cessation and 4 days late onset in 2021 resulted in 75 days reduction in LRS. Similarly, the patterns over El Gadaref in Sudan shows the 30 days delayed RCDs in 2018 with 7 days early RODs, 22 days delayed RCDs and 16 days early RODs in 2019 resulted in increased LRS with 37 days in 2018 and 38 days in 2019. In general, the RODs, RCDs, and LRS patterns of five potential agricultural sub-regions in the IGAD region examined here show reasons behind successful and failed agriculture practices. These patterns promote the cash and food crops harvest one time in Sudan and northern parts of South Sudan, 1–2 times in central Ethiopia, and 2–3 times possible farming and crops harvest over highlands of western Kenya and northern Uganda. In other words, the onset, cessation and length of season patterns are greater asserts and potential agricultural capacity over some parts of IGAD region. If utilized fully, then the food insecurity and food exports could be an issue and story of the past in the IGAD region of Eastern Africa.

4 Discussions and summary

The results from this study have shown strong connection of changes and variability in RODs, RCDs and RCDs. The mean rainfall onset, cessation dates, and length of season vary from country to country. This could be attributed to some factors modulating rainfall such as moisture, circulation conditions, prevailing winds, and teleconnections. The possible factors triggered progression of onset dates in March over Uganda to Sudan in July, March, and October in Kenya associated with the historical rain-band northward movement of ITCZ, Arabian Heat Low (Fonseca et al. 2022), moisture flues associated with Turkana low-level jet stream over Eastern Africa (Oscar et al. 2022). Other factors are Congo air mass, circulation of north-east and south-west

trade winds (Stüwe et al. 2022) and the position of the thermal equator where intense heat from the Sun. In addition, the patterns of twice mean RODs over central and northeastern Kenya during MAM and SON, unestablished RODs criteria during JJA season confirms bimodal rainfall regime over Equatorial East Africa. Also, the continued RODs from March to October over Uganda, South Sudan, highlands of western Kenya and Ethiopia confirms unimodal rainfall regimes. The thresholds for rainy day which is 1 mm and rainfall total of 20 mm over 5 days with at least 3 rain days and dry spell not exceeding 7 days in the next 21 days was found that it impossible to access the patterns of RODs over ASALs in northern Sudan, Somalia, northeastern Kenya, southeastern Ethiopia. These regions never received 20mm in three consecutive days due to nature of aridity and high rainfall variability. The areas where RODs unestablished make up majority of land, more than high percentage of East Population, home to more than 90% of the wildlife that supports the tourism industry and contributing to East Africa region GDP (Ouma et al. 2022). The 14–21 days early/delayed RODs and 21–35 days (2–5 weeks) early/delayed changes and variability in RODs coincided with severe drought and floods, increased/decreased rainfall trend over ASALs of IGAD region. For example, the late onset and early cessation in 1980s resulted in severe drought over Sudan, Ethiopia and South Sudan, and Uganda. The mean late RODs and early RCDs in 1990s and 2000s may explain the decrease in rainfall and 1998–2009 recurrent of drought events compared to the extreme wet condition triggered by early and last onset and cessation observed in recent years (2011–2020) which led to significant recovery of rainfall signals over most parts of IGAD region in recent years. In addition, the early onset and late cessation observed over most parts of the IGAD in the recent years (2011–2020) suggested the contribution of changes and variability in RODs and RCDs on extra-ordinary floods observed in 2018, 2019, and 2020 over sporadic parts of region. Also, patterns of late/early RODs and prolonged/shortened LRS explained the decreased trends of total rainfall anomalies in 1980s and 2010s. The results in this study suggested direct impacts of RODs, RCDs, and LRS on seasonal and annual total rainfall and in agreement with findings by Wainwright et al. (2019b) which revealed the contribution of changes in RODs on seasonal total rainfall patterns over eastern Africa. The author concluded the decline in MAM rainfall over East Africa is linked significantly to delayed RODs, not rainfall intensity. The decline in rainfall intensity could make it difficult to attend the 20 mm thresholds, then false RODs and unnecessary RCDs patterns. This shaded lights on failed onset and LRS thresholds in 2001 and 2002 over the Robe zone in Ethiopia during MAM season. Again, possible impacts of rainfall intensity seen clearly on patterns of RODs not established over most parts of the region in 2021 because 20 mm

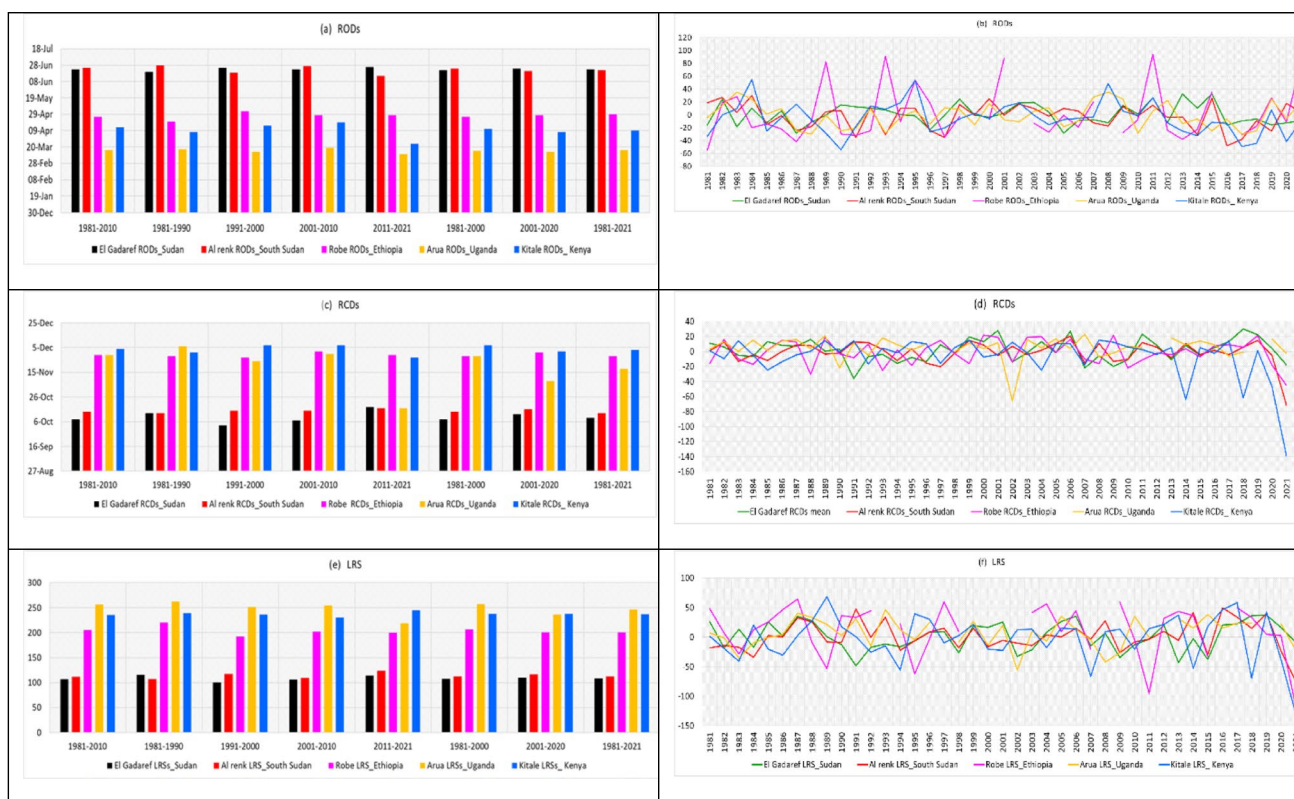


Fig. 15 Temporal trend in RODs, RCDs, and LRS in last 40 years over five potential agricultural production areas (El Gadaref in Sudan, El renk in South Sudan, Robe in Ethiopia, Kitale in Kenya, and Arua in Uganda)

over 5 days with at least 3 rain days criteria not met. Although early RODs in 2021 observed over Kitale in Kenya, but failed RCDs criteria of accumulated 10 days rainfall less than 0.5 of the evapotranspiration and not established water balance of drops below 5 mm for period of 3 days resulted in 4 months of unaccounted RCDs patterns and more than 140 days reduction in LRS in 2021. The impacts of long-term averaging of contradicting onset and cessation signals (1981–2021) reflected clearly in less than 7 days changes in RODs and RCDs. Also, variability of rainfall onset not exceeding 5% across all four seasons (MAM, JJA, SON, and DJF) over all eight IGAD member states. Therefore, it is crucial for rain-fed agriculture farmers to make decisions informed by year-to-year variation in RODs, RCDs, and LRS. The delayed rainfall cessation, which resulted in increase of length of rainy season by 14–21 days observed over greater Upper Nile province in South Sudan. In addition, northern Uganda during JJA and SON seasons could explain the role of sea surface temperature over western pacific which influence the gradual movement of ITCZ and intra-seasonal variability reported in study by Camberlin et al. (2009). The late onset and reduced LRS over most parts of region in 2011 and 2021 described the nature of relationships between east Africa rainfall patterns and

findings by Vigaud et al. (2017) which shows linked the sea surface temperatures (SSTs) over western/central Pacific, convection regimes associated with wet/dry conditions. The rainfall cessation occurred in May and December in central and northeastern Kenya, while cessation occurred in October, November, and December over Sudan, South Sudan, Ethiopia, and Uganda respectively. This implies that Uganda, Nyanza, and highlands of Western Kenya experienced cessation of rain only in December and January due to insignificant effects of seasonal-weakening of the eastern Atlantic and western Indian Ocean monsoon systems (Wainwright et al. 2019b). In addition, the character of teleconnections within the region and the dynamics associated with the Madden-Julian Oscillation which emerged as a factor in interannual and intra-seasonal variability (Nicholson, 2017). This findings explained the effects of ongoing global warming on intra-seasonal rainfall characteristics as concluded study by Gudoshava et al. (2020b), which found widespread robust changes in JJA and SON seasonal RODs, RCDs, and LRS under 1.5 °C and 2 °C GW levels over most parts of the Greater Horn of Africa. The different adaptation measures in the region may be designed based on patterns of mean, changes and variability in LRS. For example, the longest Length of rainy season in the IGAD region is observed over

most parts of Uganda and Nyanza and highlands of Western Kenya due to early rainfall in March and late cessation in December. These patterns may advance the local food production and exports if agricultural technology is put in place. The irrigation supplementary mechanisms may play a significant role over Sudan and northern parts of South Sudan, which received the majority of rain in JJA season and the LRS does not exceed 150 days (3 months). If impacts of other non-climatic factors minimize, the challenges related to food availability and accessibility through production should not be an issue over western and central Ethiopia, where LRS exceeds 150–269 days (5–7 months). Therefore, the food security agenda may be met through investments targeting the maximum use of rainfall patterns over Nyanza and highlands of Western Kenya, which has LRS range between 240 and 300 days in average due to early rainfall in March and late cessation in December. Unlike 30 counties in Kenya which observed shortening of length of season due to early withdrawal of rain (early cessation), which make it difficult to assess the length of rainy season over arid and semi-arid counties. These findings in agreement with study by Nathan et al. (2020) over the highlands of Western Kenya. These results suggest a decrease in LRS due to changes in RODs and RCDs exacerbating the food insecurity, water scarcity, and climate related conflicts observed every year. Consequently, the findings on shortening/increasing in LRS due to early/late onset and cessation may explain decline in rainfall trends, recurrent of extreme events such as drought and flood in recent years over east Africa (Omondi et al. 2014). Findings in this study suggests that planting later than April in southern and northern parts of Kenya, Somalia, South-eastern Ethiopia is likely to lead to crops, lower yields. The piece of information in this study definitely helps rain-fed agriculture, food and cash crops, ordinary farmers to make decisions on crop varieties, where and when to plant and harvest. The limitations of this study are the IGAD region characterized by variation in climatic zones and RODs, RCDs, and LRS definitions used is more suitable for agriculture and water sectors, and one definition applied for all IGAD region. Also, analyses of ROD, RCD, and LRS without considering the teleconnection and year-to-year climate fluctuation and circulation associated with warm (El Niño) and cold (La Niña) episodes.

5 Conclusions

The observed changes and variability in mean RODs, RCDs, and LRS patterns in this study mapped the important of detailed inter-annual and intra-seasonal information. It helps in timely preparations and execution of agricultural activities and food crops can be supported by a rain-fed system. The early onset and delayed rainfall cessation resulted in increase

of length of rainy season, while late onset and early cessation reduced LRS over potential agricultural areas during JJA and SON seasons. The 1980s decades observed late onset and early cessation compared to 2010s (2011–2020) decade, hence shortened LRS. This information gave insights on the needs for enhancing irrigation supplementary in the region. The mean state, early/late, increase/decreased variability RODs, RCDs, and shorter/extended LRS information in this study definitely add a new insight and helps rain-fed agriculture, food and cash crops farmers to make decisions on crop varieties, where and when to plant and harvest for sustainable food security in the IGAD region. Furthermore, observed the early onset, late cessation, prolonged/shortened LRS proofed to have a direct links with the recurrent of drought and floods and rainfall anomalies. Therefore, governments in the region has a great role to play in order to attend no poverty and zero hunger. The one of most limitations of this study is use of CHIRPS v2.0 daily which report to have large errors in estimation of variance. Further study should focus on underlying mechanisms influenced rainfall such as microscale, synoptic-scale mesoscale, and large-scale circulations on RODs, RCDs, and LRS.

Acknowledgements This work is part of a PhD work at the University of Nairobi, Kenya, Faculty of Science & Technology, Department of Earth & Climate Sciences. Also, author wish to acknowledge Climate Hazard Center, UC Santa Barbara for open access Climate Hazards Group InfraRed Precipitation with Station data (CHIRPS), and NOAA Center for Weather and Climate Prediction Climate for GTS GLOBAL gridded temperature daily which are open access from IRI/LDEO Climate Data Library, Columbia University.

Authors' contributions All authors contributed to the study conception and design. Material preparation, data collection and analysis were performed by Paulino Omoj. Omay. The first draft of the manuscript was written by Paulino Omoj. Omay supervised by Nzioka J. Muthama, Oludhe Christopher, and Josiah M. Kinama. Final manuscript version reviewed by Guleid Artan and Zachary Atheru. All authors commented on previous versions of the manuscript. All authors read and approved the final manuscript.

Funding Not applicable; however, the authors wish to acknowledge the support by Intra-ACP Climate Services and Related Applications (ClimSA) support to IGAD climate Prediction and Application Center (ICPAC) for the funds provided for the open access publication of this research.

Data Availability The secondary datasets generated during analysis are available via request. The primary data are open access from Climate Hazards Group InfraRed Precipitation with Station data (CHIRPS), Climate Hazard Center, UC Santa Barbara available via following links: [Index of /products/CHIRPS-2.0/global_daily/netcdf/p05 \(ucsb.edu\)](https://climate.geop.cam.ac.uk/products/CHIRPS-2.0/global_daily/netcdf/p05). Temperature are available as open access: GTS GLOBAL gridded temperature daily from NOAA NCEP CPC: Climate Prediction Center, open access from IRI/LDEO Climate Data Library, Columbia University available via following links: [dataset: NOAA NCEP CPC GTS GLOBAL gridded temperature daily \(columbia.edu\)](https://climate.geop.cam.ac.uk/dataset/NOAA-NCEP-CPC-GTS-GLOBAL-gridded-temperature-daily)

Data Availability Not applicable, however, we used R-Package Climate Data Tool (CDT) as software.

Declarations

I declare that this paper is my original work and has not been submitted elsewhere for publication. Where other people's work, or my own work has been used, this has properly been acknowledged and referenced in accordance with the University of Nairobi's requirements.

Consent to participate All authors consent to participate.

Consent for publication All authors consent to publish this work.

Conflict of interest The authors declare that they have no competing interests.

Open Access This article is licensed under a Creative Commons Attribution 4.0 International License, which permits use, sharing, adaptation, distribution and reproduction in any medium or format, as long as you give appropriate credit to the original author(s) and the source, provide a link to the Creative Commons licence, and indicate if changes were made. The images or other third party material in this article are included in the article's Creative Commons licence, unless indicated otherwise in a credit line to the material. If material is not included in the article's Creative Commons licence and your intended use is not permitted by statutory regulation or exceeds the permitted use, you will need to obtain permission directly from the copyright holder. To view a copy of this licence, visit <http://creativecommons.org/licenses/by/4.0/>.

References

- Amarasingha RPRK, Galagedara LW, Marambe B, Silva GLLP, Punyawardena R, Nidumolu U, Howden M, Suriyagoda LDB (2015) Aligning Sowing Dates with the Onset of Rains to Improve Rice Yields and Water Productivity: Modelling Rice (*Oryza sativa* L.) Yield of the Maha Season in the Dry Zone of Sri Lanka. *Trop Agric Res* 25(3):277. <https://doi.org/10.4038/tar.v25i3.8038>
- Camberlin P, Moron V, Okoola R, Philippon N, Gitau W (2009) Components of rainy seasons' variability in Equatorial East Africa: Onset, cessation, rainfall frequency and intensity. *Theor Appl Climatol* 98(3–4):237–249. <https://doi.org/10.1007/s00704-009-0113-1>
- Camberlin P, Okoola RE (2003) The onset and cessation of the "long rains" in eastern Africa and their interannual variability. *Theor Appl Climatol* 75:43–54. <https://doi.org/10.1007/s00704-002-0721-5>
- Chemura A, Schauburger B, Gornott C (2020) Impacts of climate change on agro-climatic suitability of major food crops in Ghana. *PLoS One* 15(6):1–21. <https://doi.org/10.1371/journal.pone.0229881>
- Cobaner M, Citakoğlu H, Haktanir T, Kisi O (2017) Modifying Hargreaves-Samani equation with meteorological variables for estimation of reference evapotranspiration in Turkey. *Hydrol Res* 48(2):480–497. <https://doi.org/10.2166/nh.2016.217>
- Dinku T, Funk C, Peterson P, Maidment R, Tadesse T, Gadain H, Ceccati P (2018) Validation of the CHIRPS satellite rainfall estimates over eastern Africa. *Q J R Meteorol Soc* 144:292–312. <https://doi.org/10.1002/qj.3244>
- Funk C, Dettinger MD, Michaelsen JC, Verdin JP, Brown ME, Barlow M, Hoell A (2008) Warming of the Indian Ocean threatens eastern and southern African food security but could be mitigated by agricultural development. *Proc Natl Acad Sci USA* 105(32):11081–11086. <https://doi.org/10.1073/pnas.0708196105>
- Funk C, Peterson P, Landsfeld M, Pedreros D, Verdin J, Shukla S, Husak G, Rowland J, Harrison L, Hoell A, Michaelsen J (2015) The climate hazards infrared precipitation with stations - A new environmental record for monitoring extremes. *Sci Data* 2(1):1–21. <https://doi.org/10.1038/sdata.2015.66>
- Gitau W, Ogallo L, Camberlin P, Okoola R (2013) Spatial coherence and potential predictability assessment of intraseasonal statistics of wet and dry spells over Equatorial Eastern Africa. *Int J Climatol* 33(12):2690–2705. <https://doi.org/10.1002/joc.3620>
- Gudoshava M, Misiani HO, Segele ZT, Jain S, Ouma JO, Otieno G, Anyah R, Indasi VS, Endris HS, Osima S, Lennard C, Zaroug M, Mwangi E, Nimusiima A, Kondowe A, Ogwang B, Artan G, Atheru Z (2020a) Projected effects of 1.5 °C and 2 °C global warming levels on the intra-seasonal rainfall characteristics over the Greater Horn of Africa. *Environ Res Lett* 15(3). <https://doi.org/10.1088/1748-9326/ab6b33>
- Gudoshava M, Misiani HO, Segele ZT, Jain S, Ouma JO, Otieno G, Anyah R, Indasi VS, Endris HS, Osima S, Lennard C, Zaroug M, Mwangi E, Nimusiima A, Kondowe A, Ogwang B, Artan G, Atheru Z (2020b) Projected effects of 1.5 °C and 2 °C global warming levels on the intra-seasonal rainfall characteristics over the Greater Horn of Africa. *Environ Res Lett* 15(3):034037. <https://doi.org/10.1088/1748-9326/ab6b33>
- Haile GG, Tang Q, Hosseini-Moghari SM, Liu X, Gebremicael TG, Leng G, Kebede A, Xu X, Yun X (2020) Projected Impacts of Climate Change on Drought Patterns Over East Africa. *Earth's Future* 8(7):e2020EF001502. <https://doi.org/10.1029/2020EF001502>
- Hietarinta J (2005) Hirota's bilinear method and soliton solutions. *Physics AUC* 15:31–37
- Kandji ST, Verchot LV (2014) Impacts of and adaptation to climate variability and climate change in the East African Community. A Focus on the Agricultural Sector. World Agroforestry Centre, Nairobi
- Kirina T, Groot A, Shilomboleni H, Ludwig F, Demissie T (2022) Scaling climate smart agriculture in East Africa: experiences and lessons. *Agronomy* 12(4):1–30. <https://doi.org/10.3390/agronomy12040820>
- Kumar U, Singh P, Boote KJ (2012) Effect of climate change factors on processes of crop growth and development and yield of groundnut (*Arachis hypogaea* L.). *Adv Agro* 116:41–69. <https://doi.org/10.1016/B978-0-12-394277-7.00002-6>
- Lobell DB, Burke M (2009) Climate change and food security: adapting agriculture to a warmer world (Advances in Global Change Research). <http://www.amazon.com/Climate-Change-Food-Security-Agriculture/dp/9048129524>. Springer Science & Business Media
- Lyon B, Dewitt DG (2012) A recent and abrupt decline in the East African long rains. *Geophys Res Lett* 39(2). <https://doi.org/10.1029/2011GL050337>
- MacLeod D (2018) Seasonal predictability of onset and cessation of the east African rains. *Weather Clim Extremes* 21:27–35. <https://doi.org/10.1016/j.wace.2018.05.003>
- Mwangi E, Wetterhall F, Dutra E, Di Giuseppe F, Pappenberger F (2014) Forecasting droughts in East Africa. *Hydrol Earth Syst Sci* 18(2):611–620. <https://doi.org/10.5194/hess-18-611-2014>
- Nathan OO, Felix NK, Milka KN, Anne M, Noah A, Daniel MN (2020) Suitability of different data sources in rainfall pattern characterization in the tropical central highlands of Kenya. *Heliyon* 6(10):e05375. <https://doi.org/10.1016/j.heliyon.2020.e05375>
- Nicholson SE (2017) Climate and climatic variability of rainfall over eastern Africa. *Rev Geophys* 55(3):590–635. <https://doi.org/10.1002/2016RG000544>
- Olatunde AF, Love JO (2018) Recent changes in onset and cessation dates of rainfall and their effects on farming activities in sub-urban areas of Lokoja. *Int J Soc Sci* 12(2):34–54
- Omoj P, Ogallo L, Oludhe C, Gitau W (2016) Temporal and spatial characteristics of the June-August seasonal rainfall and

- temperature over South Sudan. *J Meteorol*. <https://doi.org/10.20987/jmrs.5.08.2016>
- Oscar L, Nzau MJ, Ellen D, Franklin O, Rachel J, Richard W, Tom W (2022) Characteristics of the Turkana low-level jet stream and the associated rainfall in CMIP6 models. *Clim Dyn*:1–7. <https://doi.org/10.1007/s00382-022-06499-4>
- Ouma J, Opijah FJ, Muthama NJ (2022) Forage monitoring and prediction model for early warning application over the East of Africa Region Forage Monitoring and Prediction Model for Early Warning Application over the East of Africa Region. *J Atmos Sci Research* 5(4):1–9. <https://doi.org/10.30564/jasr.v5i4.4809>
- Recha CW, Makokha GL, Traore PS, Shisanya C, Lodoun T, Sako A (2012) Determination of seasonal rainfall variability, onset and cessation in semi-arid Tharaka district, Kenya. *Theor Appl Climatol* 108:479–494. <https://doi.org/10.1007/s00704-011-0544-3>
- Segele ZT, Lamb PJ (2005) Characterization and variability of Kiremt rainy season over Ethiopia. *Meteorol Atmospheric Phys* 89(1–4):153–180. <https://doi.org/10.1007/s00703-005-0127-x>
- Stüwe K, Robl J, Turab SA, Sternai P, Stuart FM (2022) Feedbacks between sea-floor spreading, trade winds and precipitation in the Southern Red Sea. *Nat Commun* 13(1):1–9. <https://doi.org/10.1038/s41467-022-32293-1>
- Uprety DC, Reddy VR, Mura JD (2019) Historical analysis of climate change and agriculture. *Clim Change Agric* :7–29. https://doi.org/10.1007/978-981-13-2014-9_2
- Vigaud N, Lyon B, Giannini A (2017) Sub-seasonal teleconnections between convection over the Indian Ocean, the East African long rains and tropical Pacific surface temperatures. *Int J Climatol* 37(3):1167–1180. <https://doi.org/10.1002/joc.4765>
- Wainwright CM, Marsham JH, Keane RJ, Rowell DP, Finney DL, Black E, Allan RP (2019a) ‘Eastern African Paradox’ rainfall decline due to shorter not less intense Long Rains. *NPJ Clim Atmos Sci* 2(1):34. <https://doi.org/10.1038/s41612-019-0091-7>
- Wainwright CM, Marsham JH, Keane RJ, Rowell DP, Finney DL, Black E, Allan RP (2019b) ‘Eastern African Paradox’ rainfall decline due to shorter not less intense Long Rains. *NPJ Clim Atmos Sci* 2(1):1–9. <https://doi.org/10.1038/s41612-019-0091-7>
- Yashim JT, Abdussalam AF, Abbas II (2020) An assessment of rainfall attributes and onsets-cessations dates effective for cropping in Lafia, Nasarawa State, Nigeria. December 2021. <https://lens.org/155-205-739-362-73X>

Publisher's note Springer Nature remains neutral with regard to jurisdictional claims in published maps and institutional affiliations.